PROBABILISTIC APPROACH TO RESIDENTIAL VAPOR INTRUSION EXPOSURE SCREENING FOR CHLORINATED VOLATILE ORGANIC COMPOUNDS: A CASE STUDY IN SAN ANTONIO, TEXAS

Jill E. Johnston

A thesis submitted to the faculty of the University of North Carolina at Chapel Hill in partial fulfillment of the requirements for the degree of Master of Science in Environmental Sciences and Engineering, Gillings School of Global Public Health.

Chapel Hill
2010

Approved by:

Dr. Jacqueline MacDonald Gibson

Dr. William Gray

Dr. Marc Serre

ABSTRACT

Jill E. Johnston: Probabilistic approach to residential vapor intrusion exposure screening for Chlorinated Volatile Organic Compounds: a case study in San Antonio, Texas
(Under the direction of Dr. Jacqueline MacDonald Gibson)

The potential for subsurface volatile chemicals to migrate through the soil and impact indoor air quality is an increasingly important exposure pathway at contaminated sites. The characterization of this pathway is highly uncertain and dependent upon many site and building-specific parameters. A probability house-by-house model, based on the Johnson-Ettinger algorithm, is developed based on the current and historic conditions of groundwater contamination of tricholorethylene and tetrachlorethylene from activities at the former Kelly Air Force Base in San Antonio, Texas. The analysis suggests that historically 5.5% of houses exceed PCE screening levels (0.41 ug/m^3) at the mean level and 85.3% at the 95th percentile; for TCE (at 0.25 ug/m^3) it is 49% and 99% respectively. The current EPA model is slightly less conservative than the new parameterization by Johnson (2005). Comparison with measured samples suggests the probabilistic model underestimates exposure. Soil properties and air exchange rates are the most input critical parameters.

To *la gente* of the Committee for Environmental Justice Action and Southwest Workers Union. *Pa' todos los que luchan por un mundo mejor y trabajan para la realización de la descontaminación y la salud de nuestro ambiente, nuestros cuerpos.* I have been endlessly inspired by the commitment, courage *y corazón* of all the community leaders, uniting to overcome insurmountable obstacles. *Gracias por todo que me enseñan y la inspiración que me dan. Ojalá que este trabajo contribuya a la lucha por justicia ambiental, la salud comunitaria y la revitalización de nuestros barrios. Siguen pa'lante.*

TABLE OF CONTENTS

LIST OF TABLES

Tables

LIST OF FIGURES

Figures

LIST OF ABBREVIATIONS

AFB	Air Force Base
BME	Bayesian Maximum Entropy
BMEGUI	Bayesian Maximum Entropy Graphical User Interface
BTEX	Benzene, Toluene, Ethylbenzene, and Xylene
C	Clay
CDPHE	Colorado Department of Public Health and Environment
CL	Clay Loam
CVOC	Chlorinated Volatile Organic Compounds
DCE	Dichloroethene
EPA	Environmental Protection Agency
GSD	Geometric Standard Deviation
JEM	Johnson-Ettinger Model
LN	Lognormal
Med	Median
PCE	Tetrachloroethylene
RIOPA	Relationship of Indoor, Outdoor and Personal Air
SC	Sandy Clay
SCL	Sandy Clay Loam
Sd	Standard Deviation
SiC	Silty Clay
TCA	Trichloroethane
TCE	Tricholorethylene
USDA	United States Department of Agriculture

VOCs Volatile Organic Compounds

LIST OF SYMBOLS

A_b = area of enclosed space below grade, cm^2

α = alpha, steady-state attenuation coefficient, unitless

C_{indoor} = contaminant concentration in indoor air (mass/volume)

C_{source} = contaminant source concentration (mass/volume)

D_{air} = chemical specific molecular diffusion coefficient in air, cm^2/s

D_{H_2O} = chemical specific molecular diffusion coefficient in water, cm^2/s

D^{eff} = effective diffusion coefficient, cm^2/s

D^{eff}_{crack} = effective diffusion coefficient through cracks, cm^2/s

$D^{eff}_{c,z}$ = effective diffusion coefficient across the capillary zone, cm^2/s

D^{eff}_{i} = Effective diffusion coefficient across soil layer *i*, cm^2/s

D^{eff}_{total} = total overall effective diffusion coefficient, cm^2/s

ΔP = indoor-outdoor pressure difference, $g/cm\text{-}s^2$

E_b = Air exchange rate (1/hr)

g = acceleration due to gravity, cm/s^2 (constant)

H_i = chemical specific Henry's law constant, unitless

k = soil permeability near foundation, cm^2/s

K_i = soil intrinsic permeability, cm^2

K_{rg} = relative air permeability, unitless (between 0 and 1)

K_s = soil saturated hydraulic conductivity, cm/s

L_{crack} = enclosed space foundation or slab thickness, cm

L_i = Thickness of soil layer *i*, cm

L_t = source-building separation, cm

M = van Genuchten shape parameter, unitless

μ = viscosity of air, g/cm-s

μ_w = dynamic viscosity of water, g/cm-s (constant)

η = fraction of foundation surface area with cracks, unitless

$Q_{building}$ = building ventilation rate, cm^3/s

Q_{soil} = volumetric flow rate of soil gas into the enclosed space, cm^3/s

R_{crack} = effective crack radius or width, cm

ρ_w = density of water, g/cm^3 (constant)

S_{te} = effective total fluid saturation, unitless

θ_m = soil moisture-filled porosity, cm^3/cm^3

θ_r = residual soil water content, cm^3/cm^3

θ_T = soil total porosity, cm^3/cm^3

θ_v = volumetric vapor content, m^3-vapor/m^3-soil

V_b = Building volume, cm^3

X_{crack} = total length of cracks through which soil gas vapors are flowing (i.e. perimeter), cm

Z_{crack} = crack opening depth below grade, cm

INTRODUCTION

Traditionally, air quality monitoring has focused on outdoor air. Since the 1970s, increasing attention has been given to evaluating indoor air quality and its impact on public health. Urban residents are known to spend 85 - 90% of their time indoors, where elevated concentrations of contaminants are commonly present, even in non-industrial settings (Klepeis et al., 2001; Spengler & Sexton, 1983). Compared to the consumption of drinking water, humans inhale 10,000 times more liters of air per day, an involuntary exposure that is not easily avoided (Schuver, 2007). It is likely that susceptible populations, including the elderly, children, those with a preexisting condition and women who are pregnant spend even more time indoors. Studies indicate that the inhalation route of exposure can lead to higher toxicities than exposures via oral routes (Pepelko & Withey, 1985). Consequently, even low levels can present human health risks over a lifetime of exposure.

There has been recognition since the early 1990s of the potential for anthropogenic chemicals to threaten indoor air quality. With growing health concern over hazardous waste sites, the EPA integrated indoor air pollution as an exposure pathway to subsurface contamination into its Superfund guidance in 1992 (U.S. EPA, 1992). Volatile organic compounds (VOCs) are reported at about one half of all Superfund and other similar hazardous waste sites. In approximately 50% of these sites, conditions are thought to favor intrusion of vapors into buildings from the contaminated groundwater (Schuver, 2007). Risk assessments at sites with contaminants in groundwater have often focused only on exposure to contaminants through the use of water for drinking,

showering or other activities. Few studies have considered exposure to contaminants via intrusion of vapors into building from groundwater plumes. Nonetheless, this scenario is commonplace in urban areas with shallow contaminated aquifers or soil. The indoor air inhalation exposure pathway significantly influences human health risk to volatile organic compounds (Ferguson, Krylov, & McGrath, 1995; M. L. Fischer et al., 1996; Little, Daisey, & Nazaroff, 1992; Provoost et al., 2009). In one study of multiple pathways, exposure to tetrachloroethylene (PCE) from soil-gas accounted for three-fourths of the total exposure to PCE – more than ingestion via drinking water, inhalation of vapor while showering, and inhalation of vapors from outdoor air (Hodgson, Garbesi, Sextro, & Daisey, 1992).

The Redfield site in Denver, Colorado brought national attention to the problem of vapor intrusion from chlorinated volatile organic compounds (CVOCs) in non-potable groundwater (Renner, 2002). Liver cancer incidence in this affected community was documented at more than twice the expected rate, and kidney cancer for females was 2.6 times the expected rate, although the reason for observed elevation was indeterminate (CDPHE, 2002). Elevated rates of kidney cancer and, to a lesser extent, esophageal cancer, were found at the Endicott site in New York, where trichloroethylene (TCE) was present indoors at levels exceeding New York state indoor air standards (5 mg/m^3), reaching 140 mg/m^3 (Agency for Toxic Substances and Disease Registry, 2006). Again, a definitive cause for the elevated cancer observations was inconclusive. While detailed case studies of vapor intrusion from CVOCs are limited and epidemiological studies even more so, indoor air with concentrations of contaminants at levels above recommended exposure levels has been attributed to vapor intrusion from CVOC plumes at several other sites (EerNisse, Steinmacher, Mehraban, Case, &

Hanover, 2009; Folkes, Wertz, Kurtz, & Kuehster, 2009; Kliest, 1989; McDonald & Wertz, 2007).

This paper will investigate exposure to CVOCs from the vapor intrusion pathway on a house-by-house level, utilizing probabilistic inputs in a screening model, at the former Kelly Air Force Base in southwest San Antonio, Texas.

BACKGROUND

When a subsurface release of CVOCs occurs near buildings, volatilization of the contaminants can result in vapor-phase contaminant intrusion into indoor air. The potential for vapor intrusion from a contaminant source is dependent on four basic phenomena: (a) the concentration of the contaminant in the groundwater (or soil); (b) the rate at which that contaminant can migrate through the soil toward the surface or building interface (which depends on both soil and contaminant properties); (c) the rate at which the contaminant is drawn into the building; and (d) the ability of the contaminant to accumulate indoors (which depends on building ventilation). Important parameters that influence vapor intrusion include soil characteristics, building characteristics (air exchange rate, foundation type, heating, ventilation and air conditioning system type) and temperature differentials between the indoor and outdoor environments (Abreu & Johnson, 2005). The characterization of vapor intrusion is complex, the pathway is incompletely understood and the screening necessitates site-specific information (Fitzpatrick & Fitzgerald, 2002; Folkes et al., 2009; Johnson, 2005).

Radon was the first chemical that received significant attention as one that can accumulate indoors via vapor transport from belowground sources. Exploring radon transport modeling, Nazaroff et al. (1987) showed that pressure-driven airflow is one of the critical processes governing transport of gas between soil and the building structure through building cracks and joints. The negative pressure differential that typically exists between the indoor and outdoor environments drives this transport (Garbesi & Sextro, 1989; Olson & Corsi, 2001).

Johnson-Ettinger Algorithm

The Johnson-Ettinger model (JEM) was the first model to combine subsurface vapor transport processes with indoor vapor intrusion to estimate indoor concentrations of contaminants in air due to subsurface vapor intrusion (Johnson & Ettinger, 1991). The output of the model is the vapor attenuation ratio, α, a unitless parameter that can range between zero and one. The ratio relates the indoor air concentration of the constituent to the concentration in the subsurface water (or soil); the higher the α value, the closer the ratio between source and indoor air is to one. The relationship between the concentration of a contaminant in indoor air to that in the groundwater is expressed as:

$$C_{indoor} = \alpha * C_{source} \quad (1)$$

where α = vapor attenuation ratio ($0 \le \alpha \le 1$)
C_{indoor} = contaminant concentration in indoor air (mass/volume)
C_{source} = contaminant vapor-source concentration (mass/volume)

The JEM couples one-dimensional steady state diffusion of volatile compounds through porous media with diffusion and advection through a building foundation into an indoor space (Figure 1). The α is estimated as follows (Johnson & Ettinger, 1991):

$$\alpha = \frac{\left(\frac{D_{total}^{eff} A_b}{Q_{building} L_t}\right) \exp\left(\frac{Q_{soil} L_{crack}}{D_{crack}^{eff} \eta A_b}\right)}{\exp\left(\frac{Q_{soil} L_{crack}}{D_{crack}^{eff} \eta A_b}\right) + \left(\frac{D_{total}^{eff} A_b}{Q_{building} L_t}\right) + \left(\frac{D_{total}^{eff} A_b}{Q_{soil} L_t}\right)\left[\exp\left(\frac{Q_{soil} L_{crack}}{D_{crack}^{eff} \eta A_b}\right) - 1\right]} \quad (2)$$

where α = alpha, steady-state attenuation coefficient, unitless

D_{total}^{eff} = total overall effective diffusion coefficient, cm^2/s

A_b = area of enclosed space below grade, cm^2

$Q_{building}$ = building ventilation rate, cm^3/s

L_t = source-building separation, cm

Q_{soil} = volumetric flow rate of soil gas into the enclosed space, cm^3/s

L_{crack} = enclosed space foundation or slab thickness, cm

D_{crack}^{eff} = effective diffusion coefficient through cracks, cm^2/s

η = fraction of foundation surface area with cracks, unitless

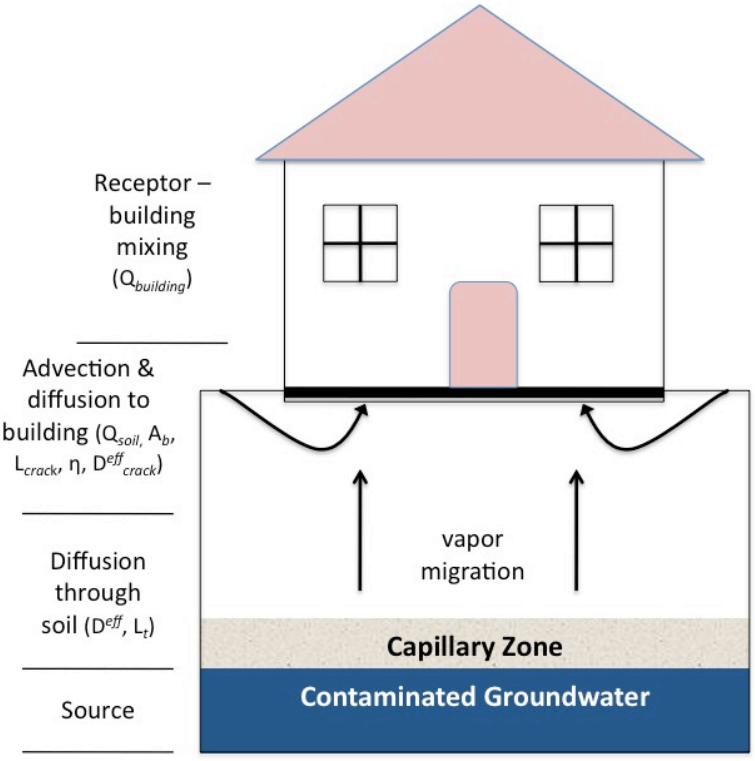

Figure 1: Conceptual model of vapor intrusion processes based on Johnson and Ettinger (1991).

The model assumes uniform and instantaneous mixing of chemicals within the building, which is represented as a one-compartment box. The transport equation is simplified through several assumptions. The partitioning of the chemical between liquid and gas phase is estimated to be at equilibrium, and Henry's Law is used to describe the expected concentration in the vapor phase. It is assumed that there is no degradation or production of the contaminant of concern indoors, which is reasonable for chlorinated

solvent species because these chemicals have relatively slow biodegradation rates. Diffusion is assumed to be the only transport process from the subsurface to the area adjacent to the building structure. VOC vapors move from the groundwater toward the land surface at a mass transfer rate based on Fick's Law, which states that the diffusive flux moves from regions of high concentration to low concentration, with a magnitude that is proportional to the concentration gradient. Since the plume is assumed to cover an area much larger than the building structure, the one-dimensional transport model, while spatially simplistic, is considered an appropriate characterization (Mills, Liu, Rigby, & Brenners, 2007). The majority of the primary inputs (Equation 2) are not typically characterized in a site assessment and are generally estimated from what is already known or with values based on previous studies. The model does not incorporate factors of spatial variations in geology, time and space variability in vadose zone transport processes, which is thought to contribute to imprecision in modeled prediction (Folkes et al., 2009).

Models, Uncertainty and Variability

Currently, regulatory agencies seek reliable approaches for determining when and where vapor intrusion can pose a health risk and for developing soil and groundwater screening levels (i.e., concentrations of contaminants in soil and groundwater that may signal the presence of a vapor intrusion risk). A mathematical screening tool is necessary due to the political, technical and monetary constraints on monitoring indoor air quality (especially in private homes) in order to identify priority sites for testing. The majority of inputs to the JEM are not easily measured, and all the processes that influence the intrusion of VOCs are still not well understood (Hers & Zapf-Gilje, 2003). There are few detailed field studies on vapor intrusion into buildings and thus few published reports of α values.

Table 1 details results from studies that measured the ratio of contaminants in the groundwater to that in the indoor air of a residence. The values range over several orders of magnitude indicating the variability between and within sites as well as the problem of merely choosing an average value to use as a screening tool. The study of vapor intrusion has yet to collect extensive data sets to refine and compare the outputs of the JEM and other vapor intrusion models. Further, current regulations do not require the consideration of uncertainty in inputs to these models and thus fail to consider how these uncertainties may affect decisions about whether control of vapor intrusion risks should be required (Environmental Quality Management, 2004). The high degree of uncertainty is partially attributed to the lack of representation by the model of the existing spatial and temporal variability that affect the dominant transport processes (Folkes et al., 2009; Provoost et al., 2009).

The sources of variability and uncertainty are not adequately captured in current vapor intrusion models. Field studies have identified spatial variability in soil-gas concentrations that do not follow a simplified homogenous site model (Bozkurt, Pennell, & Suuberg, 2009; DiGiulio et al., 2006; Eklund & Simon, 2007). Tillman and Weaver (2006) showed that the predicted cancer risk can increase by as much as 2280%, depending on the initial assumptions used in estimating the model input variables. Hers et al. (2003) suggest that, in general, the geological conditions and diffusion rates have the greatest influence on vapor intrusion processes. For example, the soil-gas advection rate is highly sensitive to soil permeability, and uncertainty increases in finer-

Table 1: Comparison of measured vapor attenuation ratios

Site	Chemical*	α, low	α, high	α, average	Source
26 vapor intrusion sites in Massachusetts (winter)	PCE	.00013	.1	.028	(Fitzpatrick & Fitzgerald, 2002)
	TCE	.00009	.097	.02	
Redfield, Colorado	CVOCs	.000013	.00034	---	(Johnson, 2002)
50 houses in Redfield, Colorado	1,1 DCE	.000001	.001	.00005 (estimated)	(Folkes et al., 2009)
5 vapor intrusion sites across county	BTEX & CVOCS	.000001	.001	---	(Hers & Zapf-Gilje, 2003)
Laboratory simulation	BTEX	.0004	.0019	---	(M. L. Fischer et al., 1996)
Endicott, New York	CVOCs	.001	.01	---	(McDonald & Wertz, 2007)
Stafford, New Jersey	BTEX	.0000043	.000012	---	(Sanders & Hers, 2006)
CDOT-MTL Denver, CO Site	TCE, 1,1-DCE, TCA	.0000048	.00034	---	(Johnson, Ettinger, Kurtz, Bryan, & Kester, 2009)
EPA draft Vapor Intrusion database (2008)	VOCs	.0000099	0.074	Median: .00011	(US EPA, 2008)

* BTEX: benzene, toluene, ethylbenzene, and xylene; PCE: tetrachloroethene; TCE: trichloroethene; DCE: dichloroethene; TCA: trichloroethane

grained soils because the influence of preferential pathways becomes more important (Hers & Zapf-Gilje, 2003). The soil moisture content values of samples adjacent to a building moderately to severely underestimate the vapor intrusion risk beneath the structure, because moisture content is generally lower underneath buildings than adjacent to them (Tillman & Weaver, 2006). However, the presence of impervious structures next to the building can increase the local soil-gas concentrations beneath the foundation (Pennell, Bozkurt, & Suuberg, 2009). It has also been found that house-to-house variability (due to differences in construction styles and ventilation rates) can

contribute up to two orders of magnitude to the variability in actual indoor air concentrations (Hers & Zapf-Gilje, 2003). Furthermore, studies have found that the accuracy of the predicted value of α depends on the availability (and quality) of site-specific data. If contamination depth is the only site-specific data available, the true α value can differ from the estimated value by three to four orders of magnitude, while the addition of soil property information can reduce the uncertainty to less than two orders of magnitude (Hers & Zapf-Gilje, 2003).

Unlike previous assumptions, recent data demonstrate that the variability and uncertainty associated with the parameters needed to estimate α tend towards a positive skew. That is, incorrect parameters will more often result in underestimation than overestimation of the actual risk (Tillman & Weaver, 2006). This uncertainty analysis used low, average and high values for input parameters which indicated that for both single and multiple parameter uncertainty analyses the outcome is skewed toward increased risk (Tillman & Weaver, 2006). The uncertainty was primarily associated with the depth to contamination, building mixing height and building air exchange rate. Tillman and Weaver (2006) explain that the α denominator is insensitive to air exchange rate and building mixing height, and the depth to contamination results in nonlinear responses in the denominator. The effect is multiplied when uncertainty from the single parameters are combined.

JEM Predictive Power

Despite the limitations of vapor intrusion modeling, the JEM is widely used for guidance on vapor intrusion in the United States and forms the basis for the screening instrument used by the EPA and 20 state agencies for volatile and semi-volatile compounds. The output is not intended to accurately predict indoor air concentration, but rather to serve

as a conservative screening-level algorithm to estimate the potential influence of groundwater contamination on indoor air and to indentify sites for further testing. In spite of critiques that JEM is too conservative, it has underpredicted the vapor attenuation ratio, and thus influence of groundwater contamination on indoor air and to identify sites in certain cases (Fitzpatrick & Fitzgerald, 2002; Hers, Zapf-Gilje, Evans, & Li, 2002; Schreuder, 2006). A comparison with 6 other algorithms that are in use in western Europe found that the JEM was the most accurate and the least conservative, as shown in Figure 2 (Provoost et al., 2009).

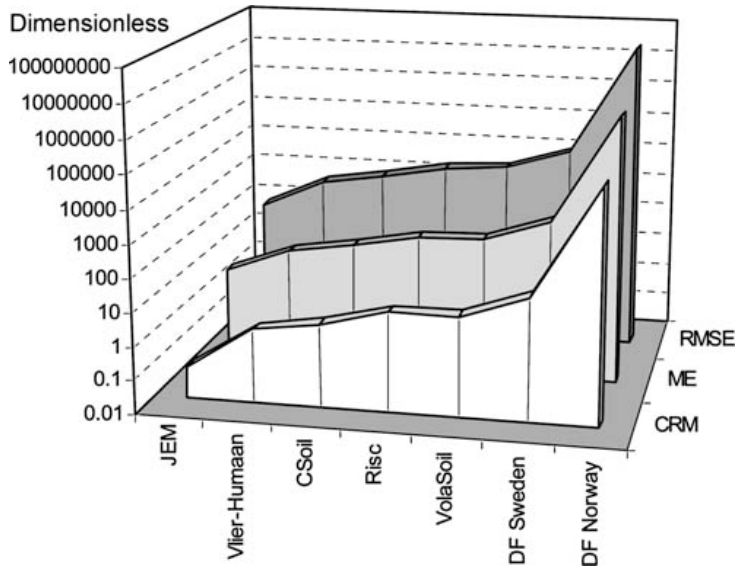

Figure 2: Ranking of statistical critical values by algorithm for indoor air. ME: maximum relative error; RMSE: root mean squared error; CRM: coefficient of residual mass (taken from Provoost et al., 2009).

Only a small number of field tests have been conducted to compare modeled estimates of α with measured values. Overall, these comparisons indicate that with reasonable input parameters the JEM can predict within one order of magnitude the expected actual indoor air concentrations (Hers & Zapf-Gilje, 2003; Johnson, 2002). While more detailed three-dimensional models exist, the level of detail and specificity required is beyond the

availability for data for this project (or for typical screening-level studies). For example Mills et al. (2007) modeled indoor air concentration with JEM at 10 μg/m^3, while the average measured value for one house was 6.3 μg/m^3 and 4.4 μg/m^3 for the other. The JEM underpredicts indoor air concentrations in cases with high advective flow rates (Fitzpatrick & Fitzgerald, 2002; Hers & Zapf-Gilje, 2003). Schreuder (2006) utilized an uncertainty-based approach, involving Monte Carlo simulations, to compare modeled versus measured α values for homes in Endicott, New York. The result indicated apparently reasonable agreement between predicted and actual distributions, demonstrating the utility of an uncertainty-based approach. However, the study also (Figure 3) shows the tendency to overpredict the frequency of low concentrations and underpredict the prevalence of high values, where mitigation needs may be greatest.

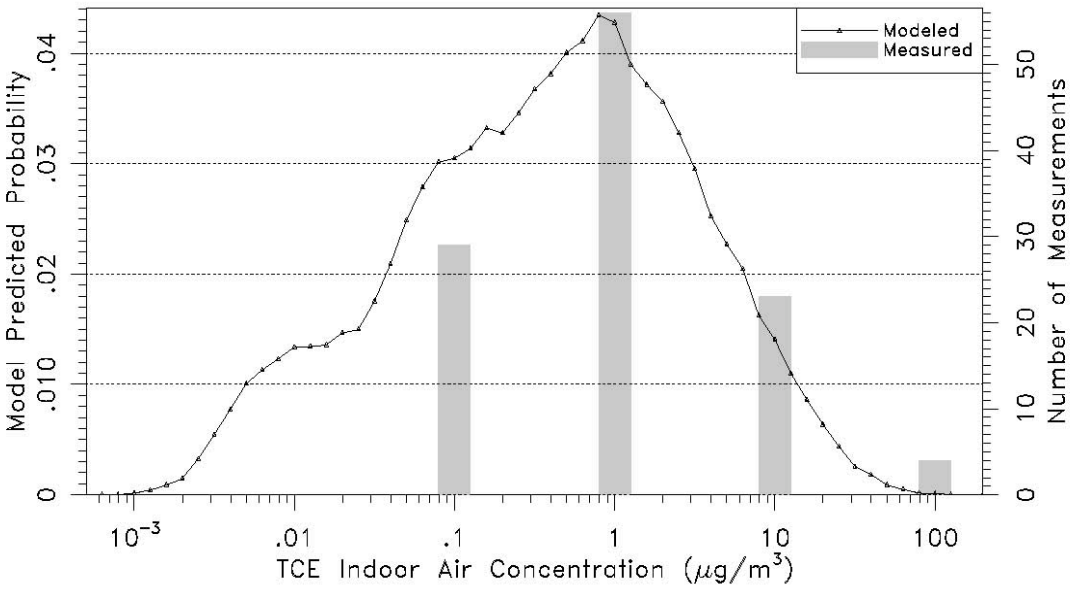

Figure 3: Modeled versus measured TCE indoor air distribution in Endicott, New York (taken from Schreuder, 2006)

Deterministic approaches do not account for the range of possible values for each input (variability) nor the uncertainty about the exact value or its distributions. Stochastic

modeling attempts to better represent both the uncertainty and variability associated with the input and output values. Two previous studies have utilized Monte Carlo simulations to account for the uncertainty and variability of the parameters used to estimate indoor air concentrations (Hers et al., 2002; Schreuder, 2006). Using probability distributions rather than fixed values for critical model parameters is important not only to represent the uncertainty in the estimated value of α but also to represent the spatial and temporal variability of α (Tillman & Weaver, 2006).

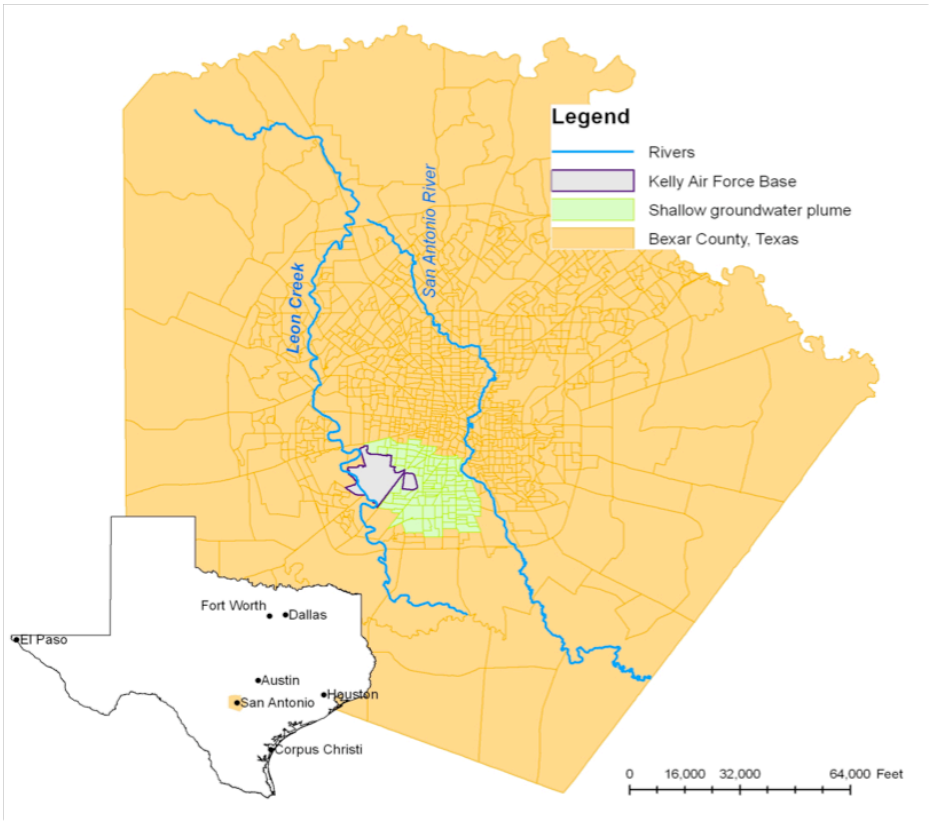

Figure 4: Kelly Air Force Base and the study area in Bexar County, Texas.

Site Description

The Department of Defense has identified, as of 2005, nearly 6000 former and current sites where the shallow groundwater has been contaminated as a result of defense activities and hazardous waste disposal and where remediation is required (Mittal, 2005). Often, the contamination has spread into adjacent neighborhoods and

community water sources. As more military bases are closed under recent Department of Defense restructuring efforts, important questions surface as to proper and effective methods to limit human exposure to and protect public health from residual contaminants.

Kelly Air Force Base operated on the southwest side of the City of San Antonio, Texas, serving as a major logistical hub for the Air Force for nearly 85 years (Figure 4). The Air Force used, stored and disposed of numerous chlorinated solvents, which consequently, migrated into the shallow aquifer. The underlying aquifer is variable and coarse-grained; typical groundwater depths are 1 to 10 meters below the surface (HydroGeoLogic, 2007). In general, the soil coarsens downward from clay to silt to sand to gravel, but the native geology has been modified by reworked or imported fill material (Bureau of Economic Geology, 1983). In 1982, the Air Force identified 27 different sites that caused groundwater contamination from activities dating back to 1940 (Radian Corporation, 1984). Prior to remediation, the contaminated plumes extended 5 miles to the southeast of the base and occupied 12 square miles. The predominant contaminants are PCE and TCE. A low-income, single-family home neighborhood surrounds the north and east of the base and sits atop the groundwater plumes.

During the initial exposure assessments, the Air Force concluded, "*Since the shallow aquifer is not used as a water supply source, contaminants in-situ have neither human health nor environmental consequences*" (Radian Corporation, 1984). Thus, the Air Force did not conduct a risk assessment to examine the potential importance of vapor intrusion. However, in 2008 and 2009, a small cohort of houses was evaluated by the Environmental Protection Agency (EPA) for an exposure route resulting from the migration of volatile chemicals from the subsurface into the indoor air of overlying

buildings. A complete exposure pathway was identified, and PCE levels exceeded the EPA human health screening levels in one-third of homes. With remedial activities underway for over a decade, current measurements cannot adequately characterize the historic risk faced by the local community residents and workers. The limited indoor air sampling that has been conducted has not adequately evaluated the current risk faced by local residents from the CVOC contamination. With cleanup time estimated at over 20 years, this risk could persist for an extended period.

METHODOLOGY

The proceeding methodology describes the procedure used to take known site-specific data coupled with information available through the literature to develop a probability-based algorithm that produces a probability distribution function for the vapor attenuation coefficient and the predicted indoor air concentration on a house-by-house basis in the potentially affected community.

Contaminant Source Data

The study area consists of the neighborhoods located to the north and east of the perimeter of the former Kelly Air Force Base. Data on the concentration of CVOCs in the aquifer and the depth below the surface from 1997-2007 were obtained from the Department of Defense Air Force Real Property Agency (AFRPA) semi-annual compliance plans for the same time range. Various private contractors for the AFRPA collected the samples, and EPA-regulated procedures were followed. Groundwater measurements came from 913 wells for a total of 3436 and 3876 samples for each TCE and PCE respectively during the study period. There were 7380 groundwater readings in total.

Method for Estimating Groundwater Concentrations at Unmonitored Locations and Times

Previous work suggests that increasing the accuracy of groundwater data will decrease the uncertainty of the JEM predictions since imprecision may be partly attributable to the spatial and temporal separation between monitoring well measured data (Folkes et al.,

2009). This study utilizes the Bayesian Maximum Entropy (BME) method to perform a spatio-temporal geostatistical analysis to estimate the concentrations of PCE and TCE in groundwater across both space and time. The observed data are only available at discrete points and times (Figure 5). This methodology allows for interpolation between these points to estimate exposures at locations and times that were not monitored. The estimation incorporates spatiotemporal information together with the monitoring data to model concentrations. Details of the methodology are available in previous studies and published books (Christakos, Bogaert, & Serre, 2001; Serre, Carter, & Money, 2004). The output is an estimated mean and variance for the PCE and TCE concentration at the center of grid cells of 500 feet by 500 feet. Residences in each grid cell were assigned groundwater concentration values drawn from a lognormal distribution with parameter for the grid cell estimated by the BME approach.

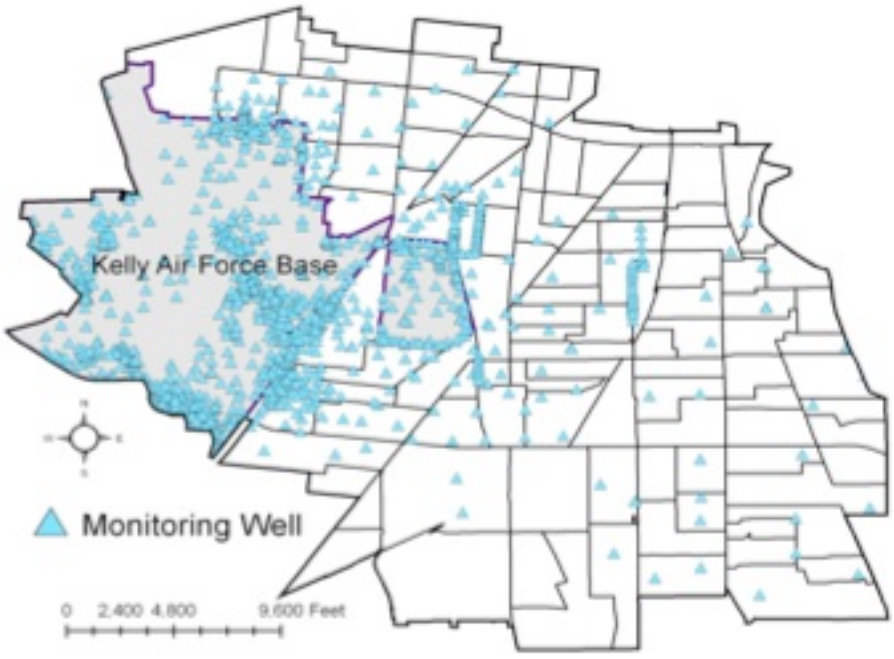

Figure 5: Location of all monitoring wells in study area.

The framework of the Bayesian Maximum Entropy utilizes general knowledge of the mean trend in the data and the spatial and temporal covariance between data points to create comprehensive space/time estimates for the concentration of PCE and TCE at any location during the study period of 1997-2007. The software BMEGUI, run in ArcGIS 9.2 finds the covariance in space-time points by identifying pairs of points and calculating the *r* and τ values for different spatial lags *r* and temporal lags τ (where lag is the distance between two points in either space or time). The result is a non-separable nested space-time covariance model characterizing the variability of the TCE or PCE in both space and time:

$$c(r,\tau) = c_1 \exp\left(\frac{-3r}{a_{r1}}\right)\exp\left(\frac{-3\tau^2}{a_{\tau 1}^{\ 2}}\right) + c_2 \exp\left(\frac{-3r}{a_{r1}}\right)\exp\left(\frac{-3\tau}{a_{\tau 2}}\right) \quad (3)$$

where $c_1, c_2, a_{r1}, a_{r2}, a_{\tau 1}, a_{\tau 2}$ are all parameters estimated from the data. For TCE, c_1 = 1.689 σ^2 and c_2 =1.0 σ^2. The sum of these two terms equals the variance of an individual space-time location. The spatial ranges are given by a_{r1} = 750 feet and a_{r2} = 3000 feet. The temporal ranges are characterized by $a_{\tau 1}$ = 5 years and $a_{\tau 2}$ = 60 years. This method is important particularly since the monitoring measurements are not synchronized in time. The model is exponential in space and exponential-Gaussian in time. The PCE covariance model follows a very similar pattern with c_1 and c_2 at 1.32 σ^2 and 2 σ^2 respectively. The spatial range is 1000 and 3000 feet and the temporal range is 7 and 60 years, for $a_{r1}, a_{r2}, a_{\tau 1}, a_{\tau 2}$ respectively.

The resulting covariance model, considered general knowledge, is then updated with the set of site-specific knowledge comprised of the monitoring data and the points in space/time (Christakos et al., 2001). The general and the specific knowledge are

combined utilizing the framework of Bayesian Maximum Entropy to produce a posterior probability distribution function for each 500 by 500 foot grid cell in the study area.

Spatial and Temporal Coverage of the Model

Routine groundwater monitoring beyond Air Force property did not begin until 1997, and thus 1998 is the earliest point in time with sufficient data to estimate concentration levels. The most recently available monitoring information is from 2007, which more closely depicts current exposure levels. This analysis includes 116 census blocks (with 600-3000 people in each block) because there was at least one monitoring well located inside of or within 1 kilometer of the boundary of each of these blocks. Seven of the 116 were eventually excluded because they did not have a sufficient number of residential homes. The analysis included 30101 homes.

Primary and Secondary Inputs to the Johnson-Ettinger Model

The Johnson-Ettinger algorithm (JEM) is derived from equations that describe contaminant partitioning between air and water phases, transport of air through the subsurface and building foundation and enclosed-space mixing (Johnson, 2005). The Millington and Quirck (1961) relationship is the basis to estimate the effective diffusion coefficients needed for the Johnson-Ettinger equation:

$$D^{eff} = D_{air}\left(\frac{\theta_v^{3.33}}{\theta_T^2}\right) + \frac{D_{H_2O}}{H_i}\left(\frac{\theta_m^{3.33}}{\theta_T^2}\right) \quad (4)$$

where D^{eff} = effective diffusion coefficient, cm^2/s

H_i = chemical specific Henry's law constant, unitless

θ_m = soil moisture-filled porosity, cm^3/cm^3

θ_T = total porosity, m^3-voids/m^3-soil

θ_v = volumetric vapor content (= θ_T - θ_m), m^3-vapor/m^3-soil

D_{air} = chemical specific molecular diffusion coefficient in air, cm^2/s

D_{H_2O} = chemical specific molecular diffusion coefficient in water, cm^2/s

The JEM equation requires estimation of three diffusion coefficients: one representing transport of soil vapor through the capillary zone, one representing transport through the vadose zone and one through the crack in the building foundation. D_{crack}^{eff} is estimated using equation 4 and assumes the cracks are filled with soil of homogeneous porosity and moisture content. For this analysis, it is also assumed that the soil in the unsaturated zone below the houses is homogenous (there is not sufficient data to accurately define soil layers and height) and thus the diffusion coefficient through the cracks and through the vadose zone is equivalent. The $D_{c,z}^{eff}$ is the effective diffusion coefficient across the capillary zone and is calculated with the air-filled porosity, total porosity and water-filled porosity specific to the capillary zone, also using equation 4. The porosity and moisture content parameters for both the vadose and capillary zones are estimated based on the Soil Conservation Service soil classification system. The van Genuchten model is used to predict the water retention parameters for the textural soil classes (van Genuchten, 1980).

The upward diffusion of contaminants is captured and carried through advective flow into the structure. Advection thus enters the equation only in the gas phase, is assumed to be the dominant transport process into the building structure and is quantified using Darcy's Law. As noted above, diffusion through cracks (but not cement itself) is also included (Tillman & Weaver, 2006). The volumetric flow rate of soil gas into the enclosed space is estimated with the given theoretical expression (Nazaroff, 1992):

$$Q_{soil} = \frac{2\pi k(\Delta P)X_{crack}}{\mu \ln\left(\frac{2Z_{crack}}{R_{crack}}\right)} \quad (5)$$

where Q_{soil} = volumetric flow rate of soil gas into the enclosed space, cm^3/s

k = soil permeability near foundation, cm^2/s

ΔP = indoor-outdoor pressure difference, $g/cm\text{-}s^2$

X_{crack} = total length of cracks through which soil gas vapors are flowing (i.e. perimeter), cm

μ = viscosity of air, g/cm-s

Z_{crack} = crack opening depth below grade, cm

R_{crack} = effective crack radius or width, cm

Equation 5 is based on pressure-driven airflow to an idealized cylinder below grade, representing the segment of the building through which the vapors pass indoors. The length of the cylinder is assumed to be X_{crack} or the perimeter of the home. Johnson (1991) expresses the equivalent radius of the floor wall seam crack as:

$$R_{crack} = \eta \frac{A_b}{X_{crack}} \quad (6)$$

where η = crack to total area ratio, unitless

A_b = surface area of enclosed space below grade, cm^2

The building ventilation rate represents ventilation throughout the indoor living space. The model assumes that the total air volume is well-mixed and the contaminant is instantaneously and homogeneously distributed. Building ventilation is calculated as:

$$Q_{building} = \frac{V_b E_b}{3600} \quad (7)$$

where E_b = air exchange rate (1/hr)

Alternative Version of the Johnson-Ettinger Model

The preceding method represents the process employed by the EPA draft guidance for vapor intrusion (2002). Johnson has more recently suggested an alternative algorithm for expressing the α coefficient that may reduce uncertainty, misuse and inconsistencies in the screening model. The algorithm can be reduced into three dimensionless groups reducing the equations to three primary parameters, given by Johnson (2005).

$$\alpha = \frac{A\exp(B)}{\exp(B) + (A) + \left(\frac{A}{C}\right)\left[\exp(B) - 1\right]} \tag{8}$$

where

$$A = \frac{D_{total}^{eff} A_b}{E_b \left(\frac{V_b}{A_b}\right) L_t}$$

$$B = \frac{\left(\frac{Q_{soil}}{Q_{building}}\right) E_b \left(\frac{V_b}{A_b}\right) L_{crack}}{D_{crack}^{eff} \eta} \tag{9}$$

$$C = \left(\frac{Q_{soil}}{Q_{building}}\right)$$

with all other variables as previously defined.

The first dimensionless group, A, represents vapor attenuation when there is no foundation or when diffusion is the controlling transport mechanism. The value of B indicates the importance of the advection process relative to diffusion in the transport of contaminants through the foundation (Johnson, 2005). C is the ratio between the vapor concentration just below the foundation and the vapor concentration indoors, assuming that advection is the dominant process. Johnson (2005) indicates that the literature

offers better insights into the selection of reasonable C values than individual Q_{soil} values and that a reasonable value for C is .001, with a potential range of .0001 to .01.

Comparison of the Two Johnson-Ettinger Models

For this case study, the EPA guidance method (hereafter referred to as the EPA model) and the new Johnson 2005 method (hereafter referred to as the JEM Alternative) are calculated separately and compared. The primary difference is the use of calculated soil vapor permeability factor and pressure differential to calculate Q_{soil} rather than the generic $Q_{soil}/Q_{building}$ ratio distribution suggested in Johnson (2005). This approaches eliminates the need to estimate the indoor-outdoor pressure differentials as well as the soil-vapor permeability.

Probability Distribution Parameters

A stochastic approach was used to implement the Johnson-Ettinger model. Based on site-specific data and previous studies, probability distributions were estimated for many of the key model inputs, listed in Table 2. When available, information from San Antonio or a similar region was used to estimate parameters. In other cases general national data or data from literature were substituted for site-specific values. The input data (both deterministic and probabilistic inputs) were incorporated into the model to generate probability distributions for the estimated indoor air concentration of TCE and PCE by house. The information was combined using Latin hypercube sampling and simulations of 800 iterations were run using Analytica software. The output is a probability distribution of α values per house. The values of α are then multiplied by groundwater concentrations estimated using BME to produce a pdf output to estimate indoor air concentrations. The analysis is run for each household in the area, based on the predicted groundwater level, chemical concentration and house volume. A sensitivity

analysis was conducted to identify the variables with the most influence on the uncertainty of the resulting estimations.

Soil Diffusion Properties

The predominant soil type was acquired from the U.S. Department of Agriculture, which uses the Soil Conservation Service classification scheme (Figure 6). Every residential land parcel was assigned a soil type. If more than one soil type was present beneath the house, then the house was assigned the soil class that occupied the greatest area. Parameters for total porosity, volumetric moisture content, residual moisture content and

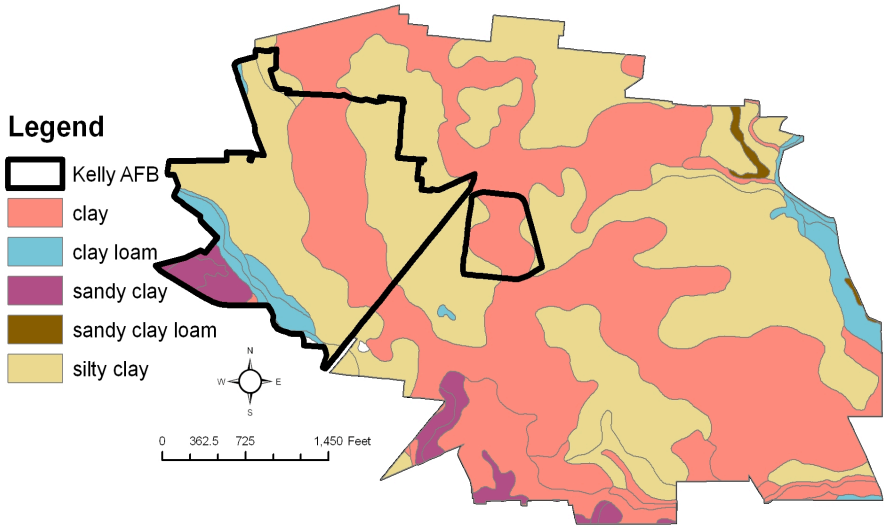

Figure 6: Native soil texture classifications in the study area (data from Soil Survey Staff, USDA, 2009).

hydraulic conductivity are available in EPA guidance documents and other literature (Carsel & Parrish, 1988; Environmental Quality Management, 2004; Schaap, 1998). Probability distributions for these soil parameters were assumed to be lognormal for this analysis. Soil air-filled porosity is the difference between total porosity and the soil moisture-filled porosity. These parameters along with chemical-specific diffusivity constants defined the effective diffusivity in the unsaturated zone (Equation 4). The

effective diffusion coefficient across the capillary zone and the height of the capillary zone were estimated based on EPA guidance for soil class averages (Environmental Quality Management, 2004). The same soil type was used for the capillary and unsaturated zones since layered information was unavailable. The total diffusivity required for Equation 2 is the sum of the diffusion properties through the capillary and the unsaturated zone, assuming homogenous soil type. The total effective diffusivity was calculated by:

$$D_{total}^{eff} = \frac{L_t}{\sum \frac{L_i}{D_i^{eff}}} \quad (10)$$

where L_i = Thickness of soil layer *i*, cm

D_i^{eff} = Effective diffusion coefficient across soil layer *i*, cm^2/s

L_t = Distance between the source of the contamination and the bottom of the enclosed space floor, cm.

Volumetric flow rate of soil gas (Q_{soil})

The pressure differential between the soil surface and enclosed space was modeled based on previous investigations that found 4 Pascal (Pa) as the average value for slab-on-grade homes (D. Fischer & Uchrin, 1996). The typical range is between 0 and 15 Pa (Environmental Quality Management, 2004; Johnson & Ettinger, 1991; Nazaroff, Lewis, Doyle, Moed, & Nero, 1987). The floor-wall seam perimeter was estimated by assuming that the length of the house was twice the width and calculating based on the known surface area. A default value of 15 cm was used to describe the crack depth below grade for slab-on-grade houses (Environmental Quality Management, 2004; P. C. Johnson, 2005). For crack ratio (η) a triangular distribution based on Johnson (2005) and Eaton & Scott (1984) was used. The soil-vapor permeability requires three

additional equations and seven more parameters. The intrinsic soil permeability is first estimated from the saturated hydraulic conductivity (Environmental Quality Management, 2004):

$$K_i = \frac{K_s \mu_w}{\rho_w g} \tag{11}$$

where K_i = soil intrinsic permeability, cm^2

K_s = soil saturated hydraulic conductivity, cm/s

μ_w = dynamic viscosity of water, g/cm-s (constant)

ρ_w = density of wager, g/cm^3 (constant)

g = acceleration due to gravity, cm/s^2 (constant)

The distribution of K_s is defined by soil class with a lognormal mean and standard deviation (Schaap, 1998). An equation from Parker et al (1987) is used to estimate the relative permeability of air and water in a two-phase system:

$$K_{rg} = (1 - S_{te})^{0.5}(1 - S_{te}^{1/M})^{2M} \tag{12}$$

where K_{rg} = relative air permeability, unitless (between 0 and 1)

S_{te} = effective total fluid saturation, unitless

M = van Genuchten shape parameter, unitless

The effective total fluid saturated is characterized by:

$$S_{te} = \frac{\theta_m - \theta_r}{\theta_T - \theta_r} \tag{13}$$

where θ_r = residual soil water content, cm^3/cm^3

and M is defined as 1-1/N, with N as another van Genuchten shape parameter, which is characterized by soil class.

Air Exchange Rate

This analysis used air exchange data from the Houston site in the national Relationship of Indoor, Outdoor and Personal Air (RIOPA) study as a proxy for the air exchange rate in San Antonio (Yamamoto, Shendell, Winer, & Zhang, 2009). The two cities lie on a similar latitude and share similar number of days of extreme heat and freezing temperatures. The air exchange rate in over 100 houses in Houston was measured (Hun, Morandi, Corsi, Siegel, & Stock, 2008; Meng et al., 2004; Yamamoto et al., 2009). The distribution of household characteristics (house size, house type, age, income, demographics) of the homes in the Houston RIOPA study matched closely with housing characteristics in San Antonio. Furthermore, unlike much of the US, the air exchange rate is lowest in the summer cooling season (Yamamoto et al., 2009). The distribution for the summer months can be considered the worst-case scenario.

Housing Square Footage, Area below grade (A_b) and Volume (V_b)

The square footage for all buildings in the area was acquired through the Bexar County Appraisal District, based on 2009 information. The information obtained included the construction year, the number of rooms and the number of stories. ArcGIS coupled these attributes with the spatial location and size of each home. Commercial, governmental and industrial sites were removed, leaving only the residential houses and the few multi-family complexes. The 30101 homes were assigned a unique identifier and independently analyzed for vapor intrusion risk in the probabilistic model. No home in the area had a basement, although some had crawl spaces. Without specific information about the height of the building, a range was used based on literature for one-story homes (Environmental Quality Management, 2004; Johnson, 2002).

$Q_{soil}/Q_{building}$ ratio

The distribution used for the $Q_{soil}/Q_{building}$ ratio was obtained from Johnson (2005), which was based on a compilation of measurements from other studies (M. L. Fischer et al., 1996; Fitzpatrick & Fitzgerald, 2002; Little et al., 1992; Olson & Corsi, 2001).

Table 2: Model inputs, parameters and references.

	Model Parameter	Description	Modeling Method*	Primary Reference
GROUNDWATER	TCE, PCE concentration	Presence of TCE and PCE in groundwater aquifer, μg/L	Bayesian Maximum Entropy, lognormal (median, GSD) for each grid cell	Air Force Real Property Agency
	L_t	Aquifer distance from ground level surface, cm	Bayesian Maximum Entropy, normal (mean, standard deviation) for each grid cell	Air Force Real Property Agency
FOUNDATION CHARACTERISTICS	L_{crack}	Foundation thickness, cm	15	(Environmental Quality Management, 2004; Johnson, 2005)
	η	Fraction of surface area with cracks, unitless	Triangular (.0005, .0038, .005)	(Eaton & Scott, 1984; Johnson, 2005; Nazaroff, 1992)
	Z_{crack}	Depth below ground surface to bottom of the foundation, cm	15	(Environmental Quality Management, 2004)
	X_{crack}	Total length of cracks through which soil gas vapors are flowing / floor-wall seam perimeter, cm	Assume house length is twice the width Length: $4\sqrt{A/2}$ Width: $2\sqrt{A/2}$	Author's judgment
HOUSE CHARACTERISTICS	ΔP	Indoor-outdoor pressure difference (Pascals)	Triangular (0,4,15)	(D. Fischer & Uchrin, 1996; Nazaroff et al., 1987; Robinson, Sextro, & Riley, 1997)
	E_b	Indoor air exchange rate (1/hr)	Annual: LN (Med: .66, GSM: .73) Summer: LN (Med: .52, GSM: .75)	(Meng et al., 2004; Yamamoto et al., 2009)
	Area (A)	Area of enclosed space below grade, cm^2	Evaluated independently for each household (discrete)	Bexar County Appraisal District, 2009
	Mixing height (to calculate V_b)	House height, cm	Triangular (213, 283, 315)	(Environmental Quality Management, 2004; Johnson, 2002)

	Model Parameter	Description	Modeling Method*		Primary Reference
SOIL PROPERTIES	θ_T	Total porosity (m^3-voids/m^3-soil)	C** CL SCL SC SiC	LN(mean: .459, sd: .09) LN(mean: .442, sd: .09) LN(mean: .384, sd: .07) LN(mean: .385, sd: .05) LN(mean: .481, sd: .07)	(Carsel & Parrish, 1988; Environmental Quality Management, 2004)
	θ_v	Volumetric moisture content (m^3-H_2O/m^3-soil)	C CL SCL SC SiC	Triangular(.098, .215, .33) Triangular(.076, .168, .26) Triangular(.063, .146, .23) Triangular(.039, .076, .10) Triangular(.11, .146, .23)	(Environmental Quality Management, 2004)
	θ_r	Residual soil moisture porosity (cm^3/cm^3)	C CL SCL SC SiC	LN(mean: .068, sd: .034) LN(mean: .095, sd: .01) LN(mean: .1, sd: .006) LN(mean: 0.01, sd: .001) LN(mean: .02, sd: .11)	(Environmental Quality Management, 2004)
	K_s	Soil saturated hydraulic conductivity, cm/day	C CL SCL SC SiC	LN(Med: 12.6, GSM: 3.55) LN(Med: 4.7, GSM: 5.01) LN(Med: 19.5, GSM: 3.47) LN(Med: 12.6, GSM: 3.55) LN(Med: 9.77, GSM: 4.20)	(Environmental Quality Management, 2004; Schaap, 1998)
	$D_{c,z}^{eff}$	Effective diffusion through the capillary zone, cm^2/s	C CL SCL SC SiC	.000016 .000048 .000026 .000007 .000026	(Carsel & Parrish, 1988; Environmental Quality Management, 2004)
	$L_{c,z}$	Height of the capillary zone, cm	C CL SCL SC SiC	81.5 46.9 25.9 30 192	(Carsel & Parrish, 1988; Environmental Quality Management, 2004)
	N	Van Genuchten curve shape parameter, unitless	C CL SCL SC SiC	LN(mean: 1.25, sd: .09) LN(mean: 1.31, sd: .09) LN(mean: 1.43, sd: .13) LN(mean: 1.21, sd: .10) LN(mean: 1.32, sd: .05)	(Carsel & Parrish, 1988; Environmental Quality Management, 2004)

	Model Parameter	Description	Modeling Method*	Primary Reference
RATIO	$Q_{soil}/Q_{building}$	Ratio of the vapor concentration just below the foundation and indoors, unitless	Triangular (.0001, .001, .01)	(Johnson, 2005)
CHEMICAL PROPERTIES AND CONSTANTS	D_{air}	Chemical specific molecular diffusion coefficient in air (cm^2/s)	PCE: 0.072 TCE: 0.079	(Environmental Quality Management, 2004)
	D_{H_2O}	Chemical specific molecular diffusion coefficient in water (cm^2/d)	PCE: $8.2*10^{-6}$ TCE: $9.1*10^{-6}$	(Environmental Quality Management, 2004):
	μ	Viscosity of air (g/cm-s)	.000179	(Environmental Quality Management, 2004)
	H_i	Chemical specific Henry's law constant at 25 C (ug/m^3-vapor)/(ug/m^3-water)	PCE: 0.753 TCE: 0.421	(Environmental Quality Management, 2004)
	ρ_w	Density of water (g/cm^3)	.9999	(Environmental Quality Management, 2004)
	μ_w	Dynamic viscosity of water (g/cm-s)	.01307	(Environmental Quality Management, 2004)
	g	Acceleration due to gravity (cm/s^2)	980.7	(Environmental Quality Management, 2004)

* LN- lognmoral; Med- median; GSD – geometric standard deviation; sd – standard deviation

** C- Clay; CL- Clay Loam; SCL- Sandy Clay; L- Loam; SC – Sandy Clay; SiC – silty clay

RESULTS

Vapor Attenuation Ratio

The first output of the model is the predicted ratio between the groundwater and the indoor air (Figure 8). A probability distribution function (pdf) is predicted for each residential home in the study region. The pdf for each home typically follows the profile of a lognormal distribution with a long tail. The pdf profile is reflective of previous studies that have shown that the majority of homes are clustered around a median value, but some can show significantly higher indoor air concentrations. Table 3 shows the summary statistics for the study region as a whole. The range of α, averaged over the study area, is typical of what has been found at previous studies sites (see Table 1) and spans just over an order of magnitude, though the median value tends toward the lower end of previous observations in the US. However, there are individual household-level cases where the α value is 100 times the community-averaged mean. The combined results from the homes demonstrate bi-model clustering of the α values; a group of homes is around 10^{-5} vapor attenuation coefficient while a larger segment is closer to $4*10^{-5}$ (Figure 11). In general, the vapor attenuation ratio for TCE is slightly higher than PCE, which can be attributed to its chemical properties, including higher diffusivities in both air and water. Comparing the two study years, the ratios are very similar, which is expected since the only differing variable is the distance from the foundation to the water table.

Vapor Attenuation Ratio Components

Through evaluating the output of each of the 3 dimensionless parameters of the JEM

Table 3: Predicted community-averaged α values from the EPA model

		Minimum	Median	Mean	Maximum	Standard deviation
PCE	1998	$5.82*10^{-6}$	$8.39*10^{-6}$	$7.61*10^{-6}$	$3.77*10^{-5}$	$7.33*10^{-6}$
	2007	*$5.72*10^{-6}$*	*$8.29*10^{-6}$*	*$8.42*10^{-6}$*	*$3.76*10^{-5}$*	*$7.52*10^{-6}$*
TCE	1998	$6.91*10^{-6}$	$1.04*10^{-5}$	$1.08*10^{-5}$	$4.39*10^{-5}$	$1.21*10^{-5}$
	2007	*$6.93*10^{-6}$*	*$1.03*10^{-5}$*	*$1.02*10^{-5}$*	*$4.23*10^{-5}$*	*$1.18*10^{-5}$*

equation (see Equation 9), insights are provided about the relative importance of various vapor transport mechanisms. Parameter B, the second dimensionless group in the JEM, in the model ranges from 1 to 95 with a mean of 16, which is a measure of the relative significance of advection versus diffusion of PCE across the foundation (Johnson, 2005). The large mean value indicates that advection plays a more important role than diffusion in driving the transport of PCE across the foundation. The results for TCE are very similar. Parameter A represents the vapor attenuation coefficient for cases where there is no foundation and, in this case, the mean value of A are predicted at $6*10^{-6}$, which is close to the averaged vapor attenuation ratio. Since this is much less than 0.1, it can be predicted that diffusion through soil is the overall rate-limiting process (Johnson, 2005). Knowledge that the native soil of the area is predominantly clay-based also anticipates that vapor movement through the soil is a limiting process.

Groundwater Chemical Concentration

As discussed in the methodology section, the Bayesian Maximum Entropy method estimates the mean value and standard deviation for the log of the concentration of each pollutant for each of the 500 by 500 feet grid cells. In both cases groundwater concentrations range over 6 orders of magnitude with peak concentration at 72000 µg/L and 54800 µg/L for PCE and TCE respectively. Off base, the highest concentrations are to the northeast of the military base. For TCE there is also a plume originating from the East Kelly Annex resulting in higher concentrations in the center region of the map. As

expected, the concentration decreases as the groundwater moves farther away from the base (Figure 8). This analysis estimated that in 1998, 99% of the houses sat above groundwater with a mean concentration exceeding the EPA Maximum Contaminant Level of 5 μg/L in groundwater for both PCE and TCE. In 2007, the number of residences were 97% and 93% for PCE and TCE respectively. For a detailed description of the methodology and outputs, refer to Appendix A.

Table 4: Summary Statistics of Groundwater data

	PCE (μg/L)		**TCE (μg/L)**		**Groundwater feet below surface (ft)**
	Raw data	*Log-transformed data*	*Raw data*	*Log-transformed data*	
Number of measurements	3436	--	3876	--	7380
Mean	111.05	1.29	31.17	1.31	17.57
Minimum	.10	-2.3	.10	-2.3	0
Maximum	72000	11.2	54800	10.9	40
Standard deviation	1704.96	1.94	1371.65	1.72	7.17
Skewness	35.05	1.51	29.4	1.13	-0.08

Estimated Indoor Air Concentrations

As suggested by previous studies, this model indicates a great deal of variability in the predicted indoor concentrations across the community, a variability that is not adequately captured with a single-point estimate for the entire region. In general, predicted concentrations of TCE indoors were higher than PCE. Figure 7 shows a histogram of the mean predicted indoor concentrations with the frequency displayed on a logarithmic scale. The range for both chemicals extends over two orders of magnitude. While the majority of the predictions cluster around low levels, considering the size of the study population, there are still a significant number of homes with indoor

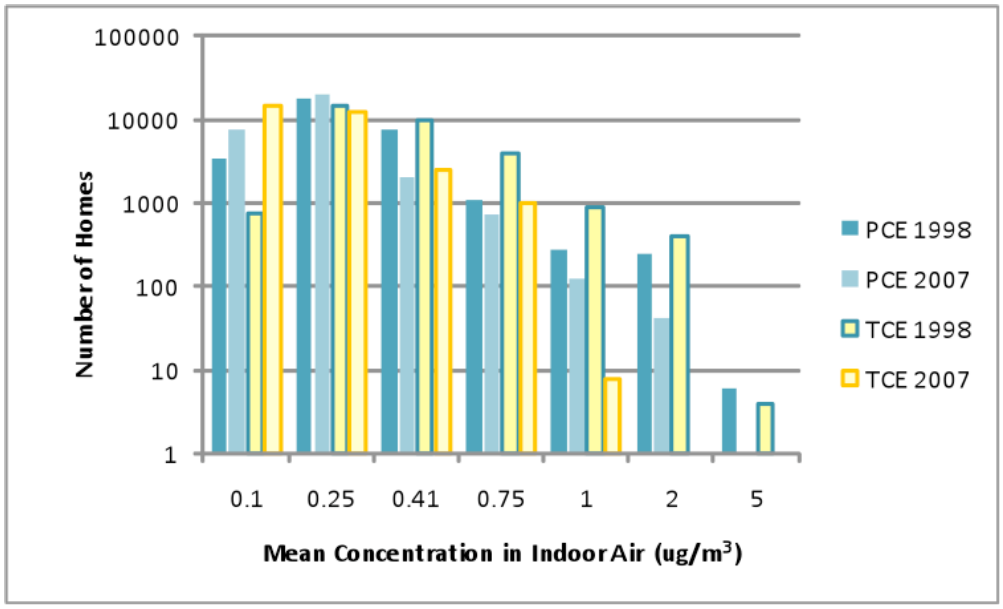

Figure 7: Frequency analysis of the mean predicted indoor air concentrations (µg/m^3).

air modeled above screening-level values. The indoor air screening level threshold established by the EPA Region 6 (including the state of Texas) is 0.41 µg/m^3 for PCE. This is based on a 1 in 10^6 increase in risk for cancer. The threshold for TCE is still under review by EPA, but the latest data indicates a level of 0.25 µg/m^3 for a 1 in 10^6 increase in cancer risk (primarily due to kidney cancer) based on research by Charbotel et al. (2006).

The risk ratio is estimated by:

Risk ratio: Predicted indoor air concentration / EPA threshold level (14)

The mean risk ratio is the ratio of the mean estimated indoor air concentration in each home divided by the EPA screening level. The 95th percentile is the ratio of the 95th percentile value in each home divided by the screening level.

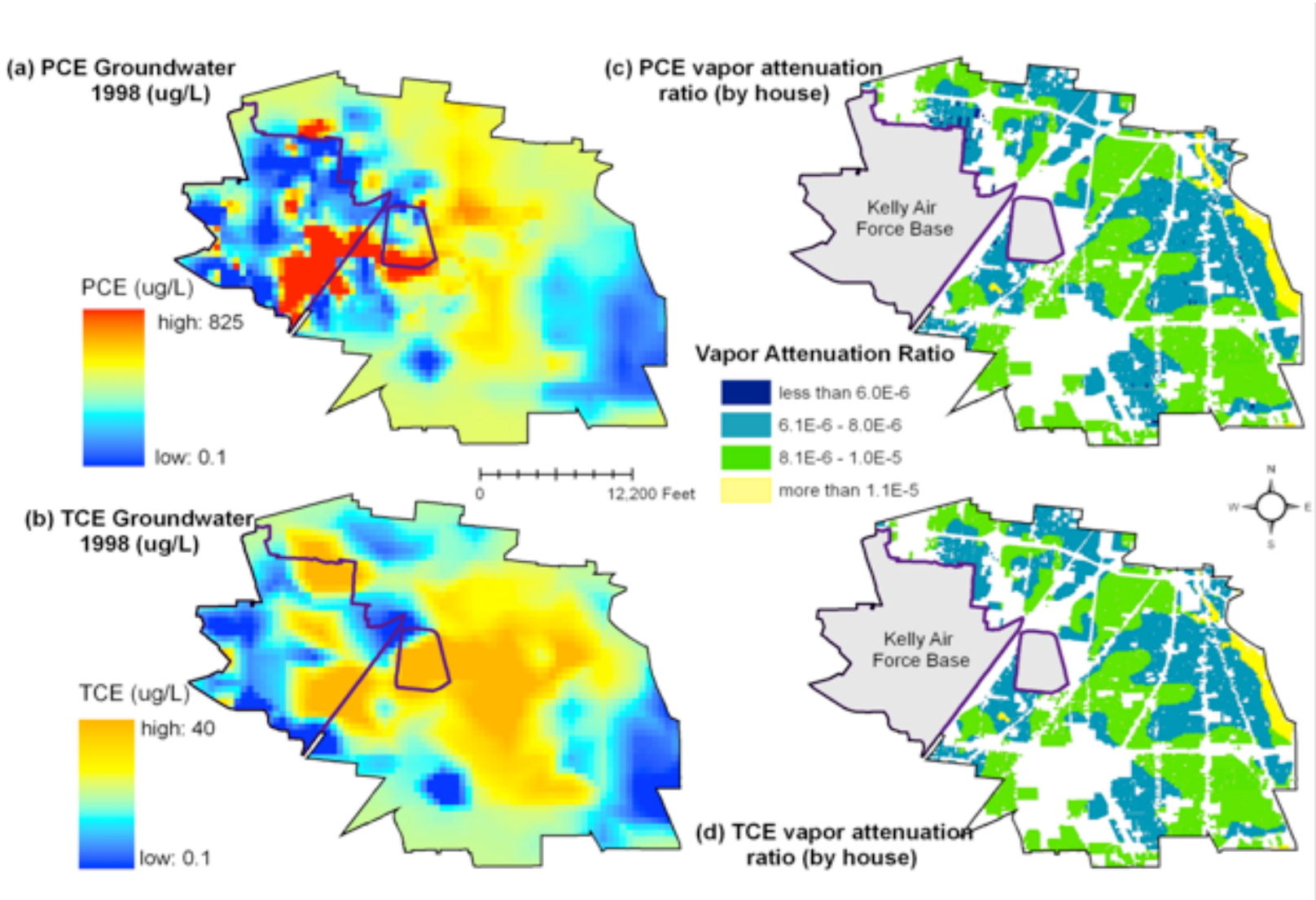

Figure 8: Estimated groundwater chemical concentration and vapor attenuation ratio. (a) Estimated PCE (ug/L) concentration in groundwater in 1998; (b) PCE vapor attenuation ratio by house; (c) Estimated TCE (ug/L) concentration in groundwater in 1998; (d) TCE vapor attenuation ratio by house.

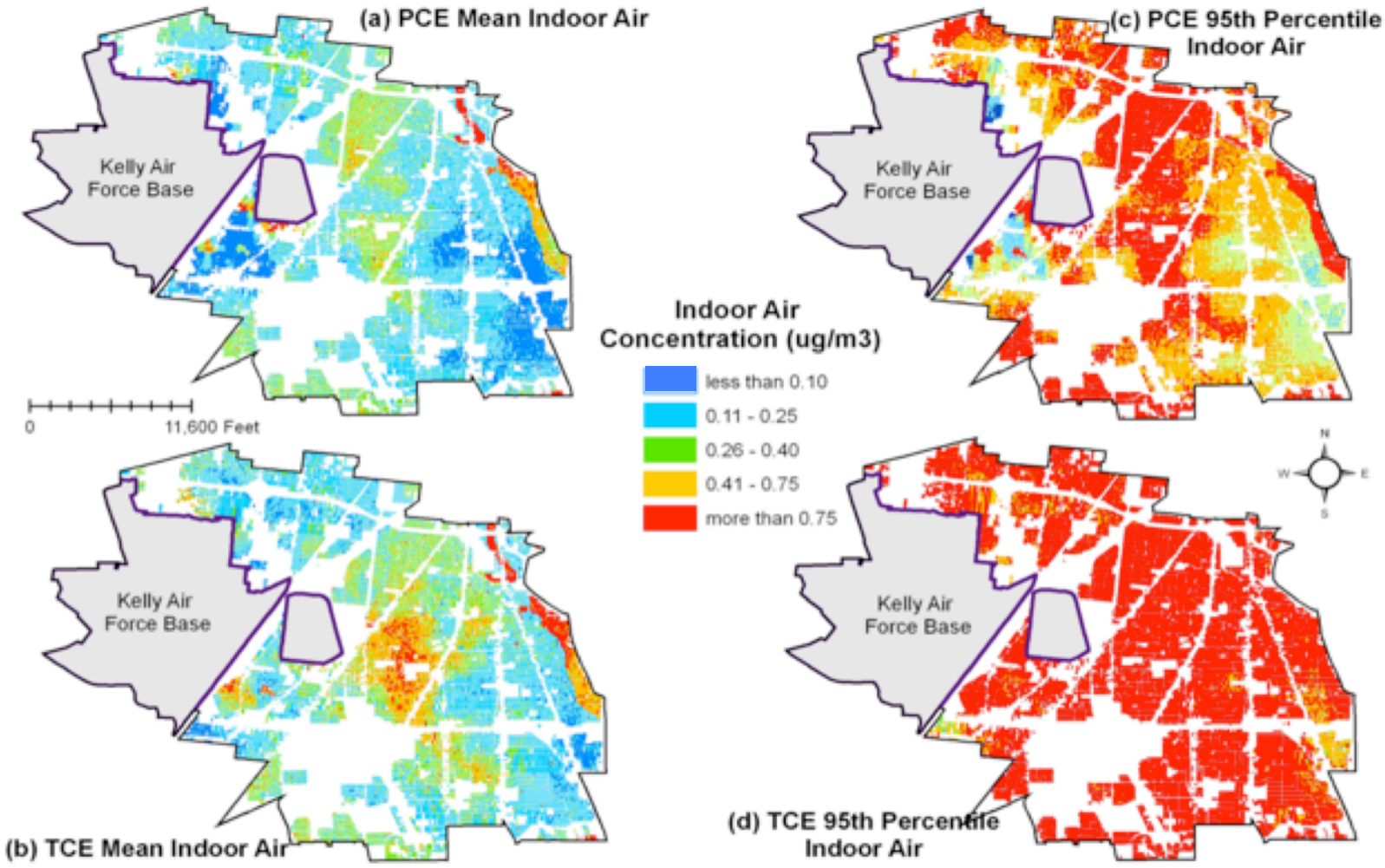

Figure 9: Modeled indoor air concentrations. (a) PCE (ug/m^3) mean estimated indoor air concentrations in 1998; (b) PCE (ug/m^3) 95th percentile estimated indoor air concentrations in 1998; (c) TCE (ug/m^3) mean estimated indoor air concentrations in 1998; (b) TCE (ug/m^3) 95th percentile estimated indoor air concentrations in 1998.

Since groundwater chemical monitoring beyond the AFB perimeter did not begin until 1997, data from 1998 is the best available proxy for historical concentration, although it is likely that the groundwater concentrations were higher in the past. These results suggest that TCE vapor exposure inside homes may present a widespread risk to the households above the Kelly AFB groundwater plume. Elevated risk to PCE is less prevalent, but, nonetheless, involves numerous homes (and people) in absolute terms. The number of homes exceeding this screening level risk threshold is presented for the mean and the 95th percentile in Table 5.

Table 5: Predicted number of homes exceeding screening levels by chemical and year.

	1998		2007	
PCE (homes above risk ratio of 1)	*Mean*	*95th percentile*	*Mean*	*95th percentile*
EPA Model	1644 (5.5%)	25688 (85.3%)	880 (2.9%)	20740 (68.9%)
JEM Alternative	2079 (6.9%)	26260 (87.2%)	1184 (3.9%)	21823 (72.5%)
Summer EPA Model	10261 (34.1%)	29099 (96.7%)	3730 (12.4%)	27193 (90.3%)
TCE (homes above risk ratio of 1)	*Mean*	*95th percentile*	*Mean*	*95th percentile*
EPA Model	14859 (49.4%)	29992 (99.6%)	3469 (11.5%)	23595 (78.4%)
JEM Alternative	16419 (54.5%)	30007 (99.7%)	3833 (12.7%)	24583 (81.7%)
Summer EPA Model	26140 (86.8%)	301010 (99.9%)	8065 (26.8%)	28917 (96.1%)

The spatial distribution of risk suggests several correlations based on the visual patterns of high estimated indoor air concentrations. First, regions with the highest groundwater concentrations present higher indoor air concentrations, particularly those closest to the perimeter of the base. However, the overall indoor air trend did not follow the groundwater trend, suggesting that concentrations alone are not a sufficient predictor of exposure. Secondly, regions with more sandy soil (or a smaller percentage of fine particles) estimate higher indoor air concentrations. The combinations of either of these two factors with a shallow groundwater table can also increase the likelihood of

high indoor concentrations of TCE and PCE. The strip along the eastern border of the study region showed the largest concentration of at-risk homes despite its distance from the contaminant source. This is likely attributed to the presence of sandy loam soil in this region, as it is situated adjacent to the San Antonio River. The soil-vapor permeability is higher particularly compared to the clay-rich soil typical of the area. Thus soil type appears to be a strong indicator of vapor intrusion risk, a finding echoed in previous studies (Bozkurt et al., 2009; Hers & Zapf-Gilje, 2003; Pennell et al., 2009; Tillman & Weaver, 2006). Variations in soil characteristics are known to contribute greatly to the output on uncertainty related to solute transport (Carsel & Parrish, 1988). The soil type is known to vary greatly based on studies on the former Kelly AFB (AFRPA, 2005), so it may not be appropriate to use the USDA soil classification as a proxy for soil type directly beneath the foundation, as it may be altered significantly (including importing of soil and/or gravel) during construction. As shown in Figure 10, the clay loam and sandy clay loam soil type on average have a vapor attenuation ratio that is an order of magnitude higher than the clay and silty clay varieties. Garbesi et al. (1983) found, however, that measured soil gas intrusion rates were actually higher than predicted, which was partially attributed to the existence of high-permeability flow paths, a phenomenon not appropriately captured in current mathematical models.

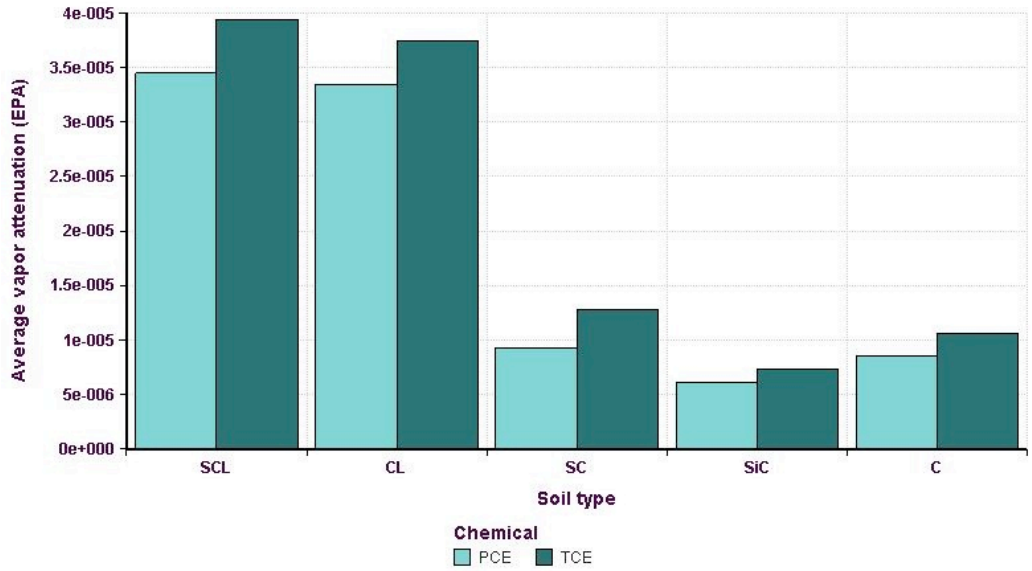

Figure 10: Averaged vapor attenuation ratio by soil type.

Comparison Between the Modeling Approaches

The previous results are all based on the predictions from the EPA version of the JEM. The model was also run using an updated version of the JEM suggested by Johnson (2005). The results generally indicated that the JEM Alternative version was slightly higher and thus more conservative (predicts a higher attenuation ratio) than the EPA version (Figure 11). The JEM Alternative does not require site-specific soil vapor permeability calculations and thus the ratio represents the range of clays, loams and sandy soils. It follows that the San Antonio site would have slightly lower than average Q_{soil} values due to the prevalence of clay. Twenty to thirty percent of the Q_{soil} to $Q_{building}$ ratio (depending on the soil texture) from the EPA model fell below the lower end of the expected distribution, that is below 10^{-4}. However, approximately three-fourths of the values fell within the generic distribution.

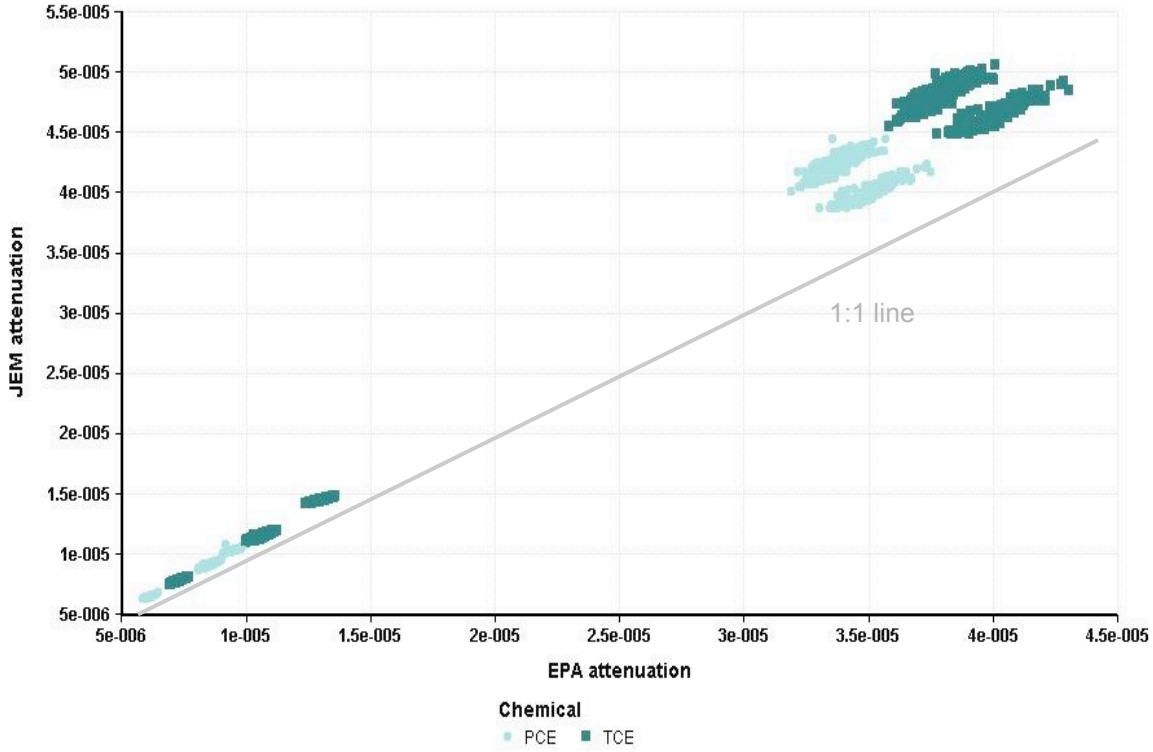

Figure 11: Comparison of the vapor attenuation ratio of the EPA and the JEM Alternative model.

Summer scenario

Due to the importance of the air exchange ratio on predicting the vapor attenuation coefficient, the model was based on air exchange rates during the summer season. Unlike other regions of the country, the air exchange values are lowest in the summer in San Antonio, representing the 'worst case scenario' for CVOC indoor air concentrations. As shown in Table 5, a reduction in the mean air exchange rate to reflect conditions during the summer time results in a five fold increase in homes at risk (at mean concentration) for PCE and a doubling for TCE in 1998. This further indicates the significance of the air exchange rate as an important predictor of indoor air quality and suggests the need to develop more site-specific and house specific estimates to improve upon the models predictive ability and identify homes at risk.

Sensitivity and Uncertainty Analysis

Sensitivity analysis evaluates how a change in the input value or assumption changes the output. The JEM is nonlinear and thus its response to changes in parameters is also nonlinear. Prior analysis shows that, in order of significance, the effective water saturation, air exchange rate, total porosity, building mixing height, and source depth have the greatest effect on predicted attenuation (Tillman & Weaver, 2006). Based on the predicted transport characteristics, Johnson (2005) suggestions that the critical (most sensitive) parameters are distance to the aquifer, effective diffusion coefficient, air exchange ratio and the ratio between volume and house area (i.e. height). For the sensitivity analysis, the change in the mean of α was predicted for each uncertainty variable at its 5th and 95th percentile value. The results shown in Figure 12 (for PCE in 1998) indicate that the air exchange rate has the largest influence on the α value. The lower the exchange rate, the higher the vapor attenuation ratio, which can vary by an order of magnitude. Air infiltration affects indoor air quality because insufficient

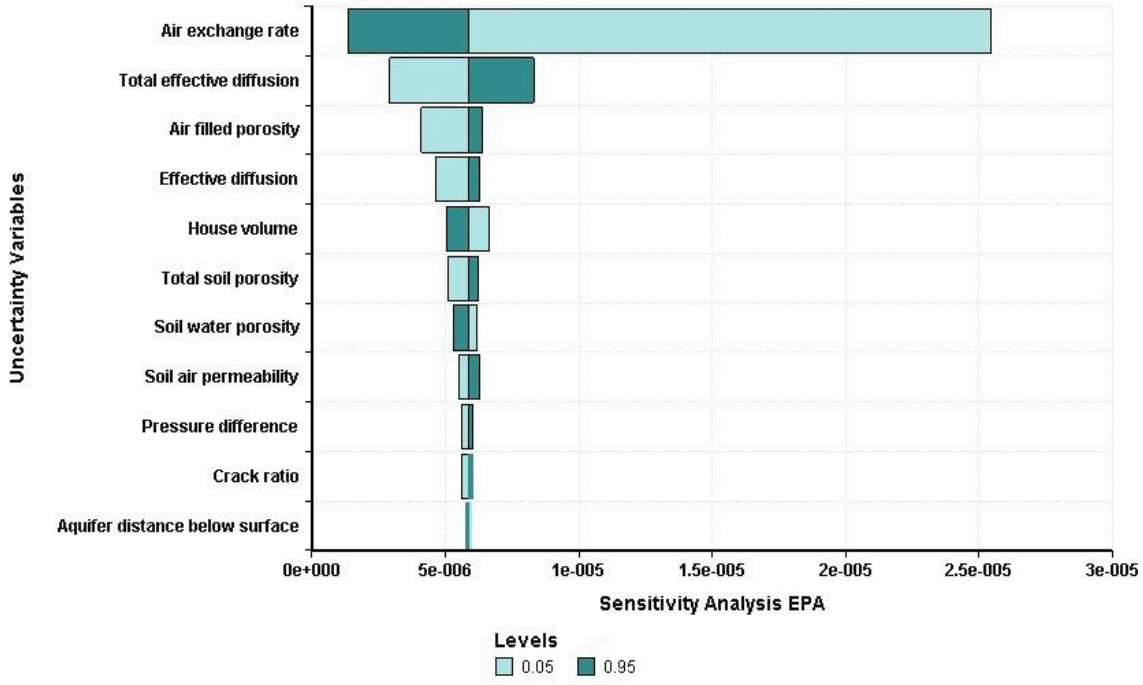

Figure 12: Sensitivity analysis of uncertainty variables in EPA JEM model (per home).

air exchange with the outdoors can lead to higher exposure to pollutants of indoor or subsurface origin (Chan, Nazaroff, Price, Sohn, & Gadgil, 2005). An uncertainty analysis, which attributes the relative importance of input uncertainty to the total uncertainty of the output, shows that 90% of the uncertainty in the model is due to the air exchange rate. (The effect of inaccurate characterization of soil texture is not included in the analysis.) The attenuation coefficient is less sensitive to the other uncertainty variables. This suggests that it is important to accurately characterize the exchange rates since the results are sensitive to this input. The other important variables include the total effective diffusion coefficient and the air-filled porosity. The model is relatively insensitive to building foundation properties, similar to other analyses (Hers & Zapf-Gilje, 2003).

When analyzing the two inputs required for the indoor air calculations, the output is twice as sensitive to the groundwater concentration compared with the vapor attenuation ratio. The range of the groundwater probability distribution is much greater than for the vapor attenuation ratio.

Comparison with Measured Values from an EPA Study

An EPA study collected a small sample of indoor air measurements in May 2008 and February 2009 from homes located near the Base (Figure 13). It included 15 measurements for PCE and 21 for TCE. These results, the only data on indoor air concentrations in homes, were compared with the modeled prediction. All homes were located near the perimeter of the base and built atop silty clay soil. As shown in Figure

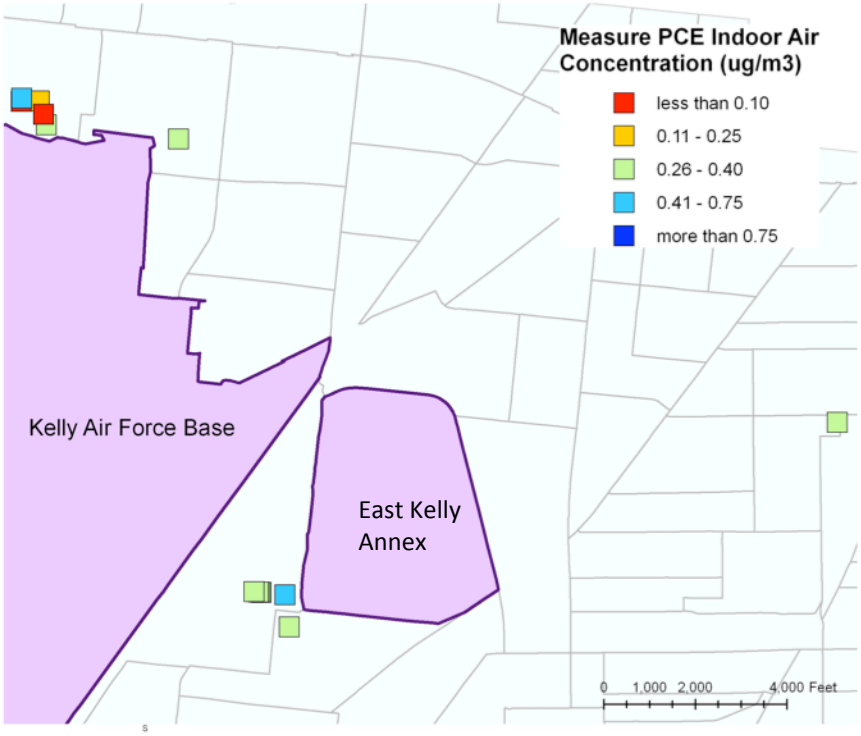

Figure 13: Map of locations of measured PCE indoor air concentrations.

14 and 15, both the EPA and JEM Alternative models consistently underpredicted measured values for PCE, although the measure value typically fell within the 95% confidence interval and all were within the range of predictions. The majority of the homes exceeded the screening level for PCE in indoor air. On average, the predicted concentrations are five times lower than measured values. At the 95th percentile, the underprediction was nominal. The use of the summer air exchange rates in the model resulted in the best matched with the measured PCE data. The model demonstrated increased accuracy for TCE, however the measured values were typically at or below the screening risk level (Figure 15). The model underpredicted by approximately 130%. The JEM Alternative and summer air exchange rates scenarios generally predicted just slightly higher than measured values for TCE. At lower levels, the model appears to be more predictive. This pattern follows the work of Schreuder (2006) in New York were

the modeled output underestimated high concentrations and overestimated the frequency of low values. In general, the prediction was within one order of magnitude accuracy.

This comparison, through limited by the quantity of measured data, points to two insights. First, parameters for the soil properties were based on native soil type national data. This fails to include changes in soil permeability and porosity due to construction, such as the addition of sand or gravel to the soil type. It also does not capture preferential pathways that may be important source of soil vapor intrusion, such as sewage pipelines. This model assumes homogenous soil type, while studies on base have shown the heterogeneity of the soil, particularly on sites with building construction. Other geological heterogeneities could be unaccounted for in the model. While a continuous clay layer has retardant effect, a discontinuous has far less of effect in reducing indoor concentrations (Bozkurt et al., 2009). On site measurements of soil properties, including permeability and better characterization of geological features in the community, would likely improve the predictive capacity of the model. Other studies suggest that this algorithm likely predicts lower than actual water-filled porosity in soil, resulting in conservative diffusion estimates (D. Fischer & Uchrin, 1996; Hers & Zapf-Gilje, 2003).

Since this model improves on the spatial resolution of the screening prediction and decreases the uncertainty associated with groundwater level and contaminant concentration, the air exchange rate becomes the critical variable. In order to refine a house-by-house approach, it is necessary to develop tools or local measurements of the indoor air exchange rate to better characterize household risk.

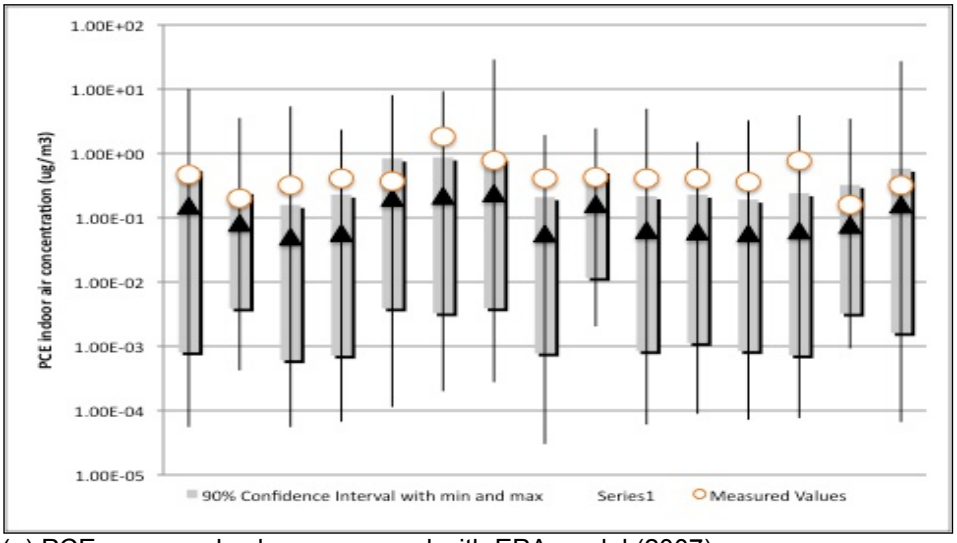

(a) PCE measured values compared with EPA model (2007)

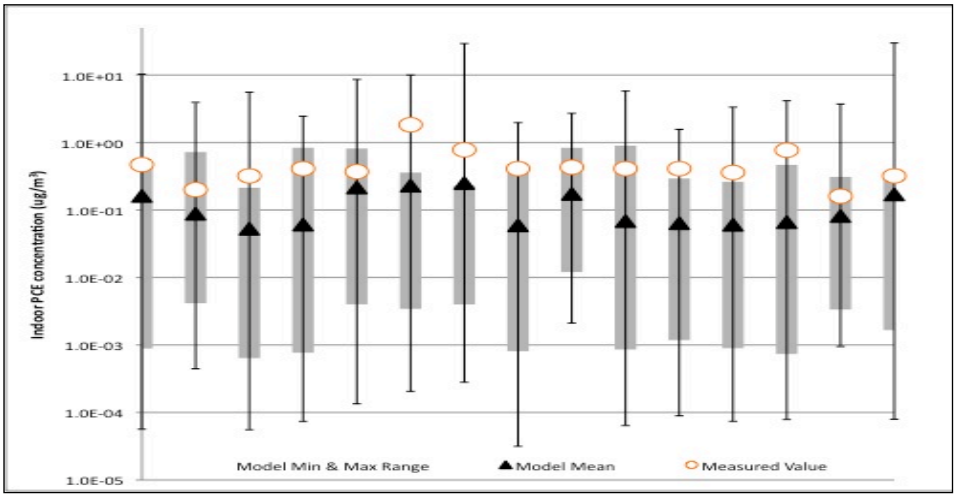

(b) PCE measured values compared with JEM Alternative model (2007)

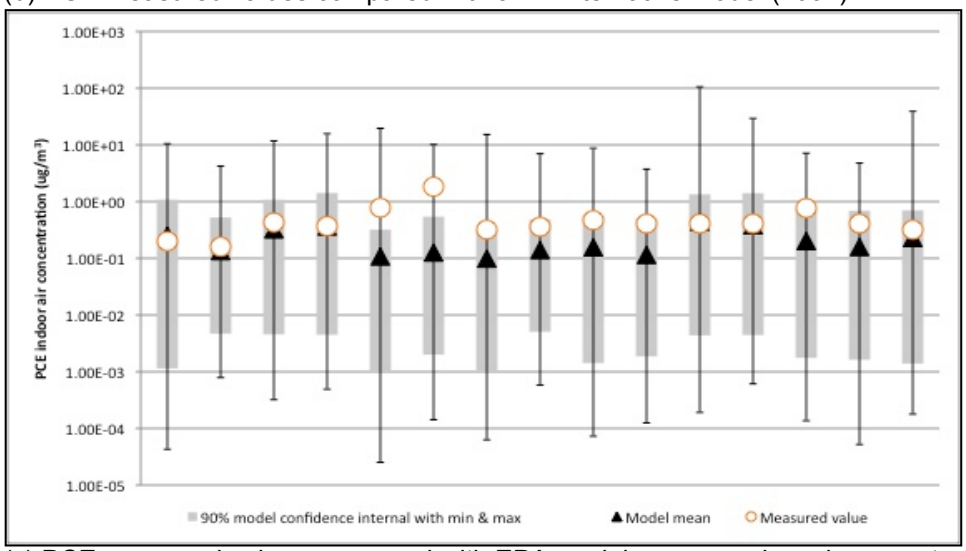

(c) PCE measured values compared with EPA model, summer air exchange rate (2007)

Figure 14: Comparison of measured data with PCE model under 3 scenarios.

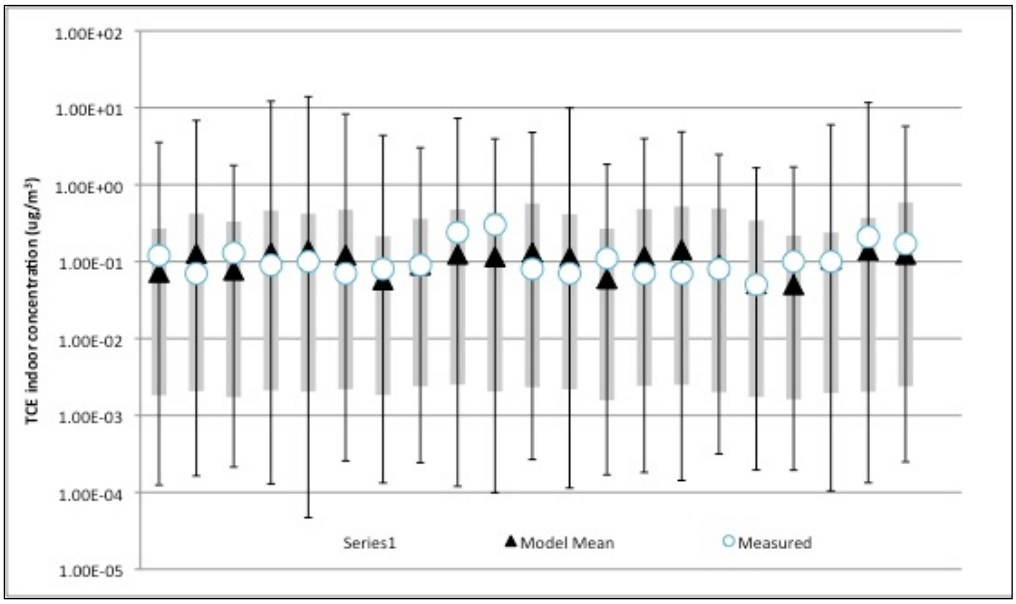

Figure 15: Comparison of measured TCE indoor air concentration with EPA predicted model values in 2007.

CONCLUSION

This analysis presents a framework by which to identify houses that are currently and were historically most at risk to the vapor intrusion exposure pathway, providing a more spatially detailed approach than the traditional community-average estimates. The model developed in this work can be a tool to better evaluate spatial distribution of potential exposure over a large community. It attempts to decrease the uncertainty of groundwater chemical concentrations and aquifer level through the use of Bayesian Maximum Entropy methodology to increase the spatial resolution at the site. In this case, the model puts an area situated at the edge of the groundwater plume at highest risk to the vapor intrusion pathway due to the underlying soil type, houses which would likely otherwise be overlooked from study. The method attempts to capture the temporal and spatial variability typically seen at other sites with vapor intrusion risk. The approach allows for analysis of alternative scenarios and the output is a range of values rather than a single value. The distribution most likely provides a more complete picture that incorporates the uncertainties and the variability at the site. Compared with the known measured values, this model seems to systemically underestimate high exposures, at least at homes atop fine grain soils and suggests that use of the 95^{th} percentile may more accurately screen for potential indoor air exposure risk. The JEM Alternative, which requires fewer inputs, particularly in terms of soil properties, closely resembles the EPA output and is in this case only slightly more conservative than the EPA model and actually closer to known indoor air values using simpler and fewer inputs. This work reiterates the importance of identifying appropriate soil parameters as well as demonstrates the need to more accurately characterize air exchange rates in order to develop a tool to analyze house-by-house risk. Finally, this analysis

concludes that the homes sitting above the shallow groundwater plume of PCE and TCE were historically and are currently at risk of vapor intrusion, particular as the chemical concentration is very high, the soil type has fewer fine particles and/or the air exchange rate is low. This modeling approach may prove increasingly useful as more sites are identified as at risk for vapor intrusion because this approach can better identify priority areas and high risk areas for further sampling.

APPENDIX A: Bayesian Maximum Entropy Modeling (for PCE)

1. Exploratory Data analysis:

(a) Histogram of raw data in log-space

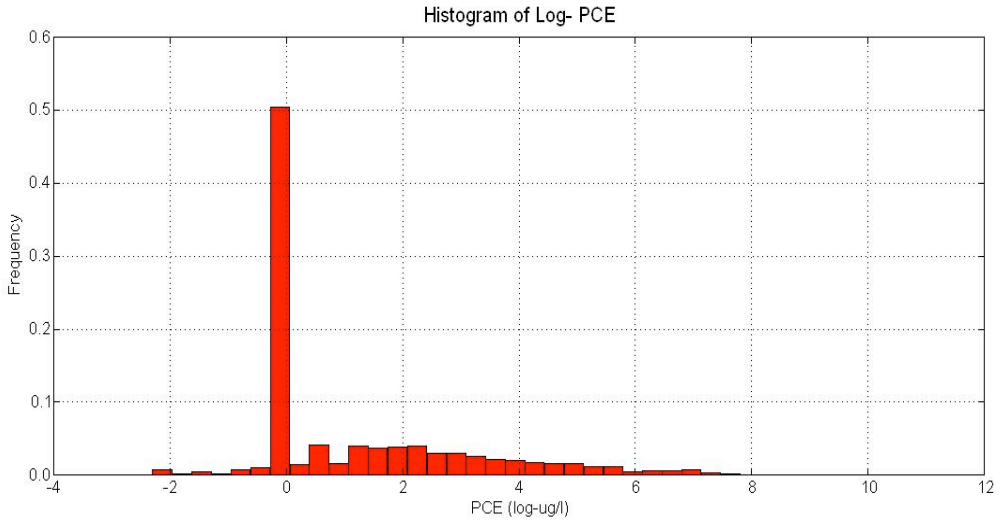

Figure A- 1: Histogram of raw log-transformed data for PCE groundwater measurements from 1997-2007.

(b) Temporal Variation of PCE concentration for 4 well locations. The well on base, near the principal source of PCE shows concentrations increasing over time. The two wells near the base perimeter (north and southeast) on average decline over time while the well 3 miles east of the base shows little variation during the study period.

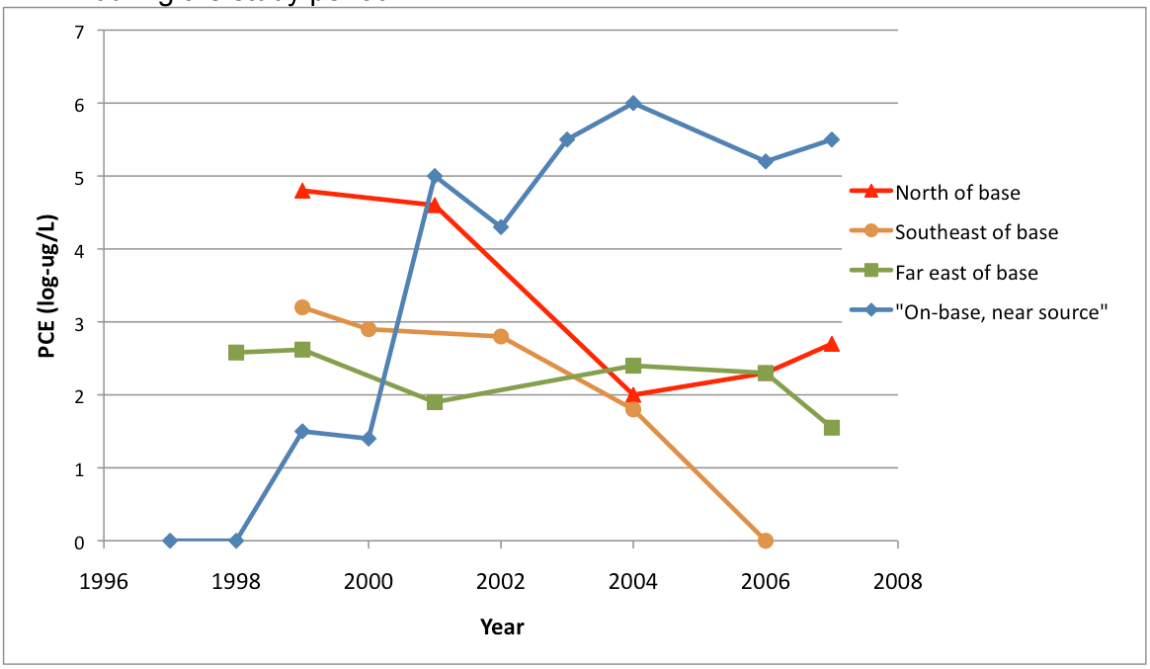

Figure A- 2: Temporal trends of PCE concentration in groundwater for four monitoring wells, located throughout the study region.

(c) The spatial distribution of groundwater measurements and concentrations in 1998 and 2007 for PCE (aggregated over one year).

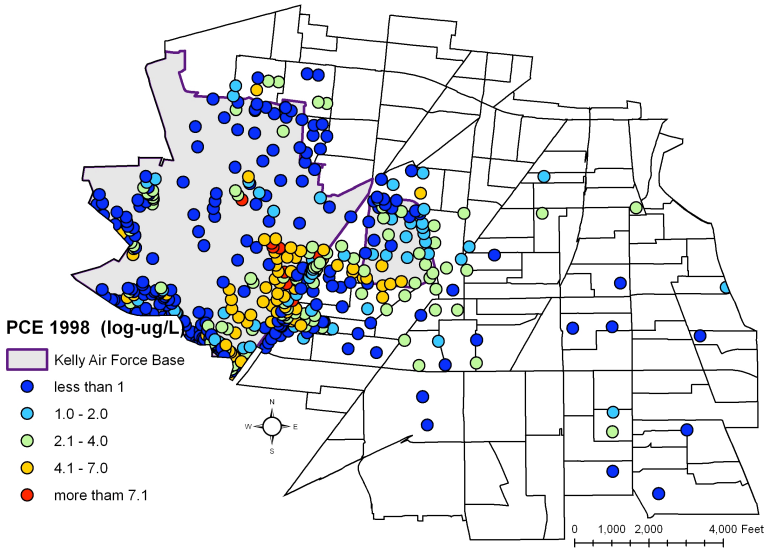

Figure A- 3: Spatial distribution of PCE well measurements in 1998.

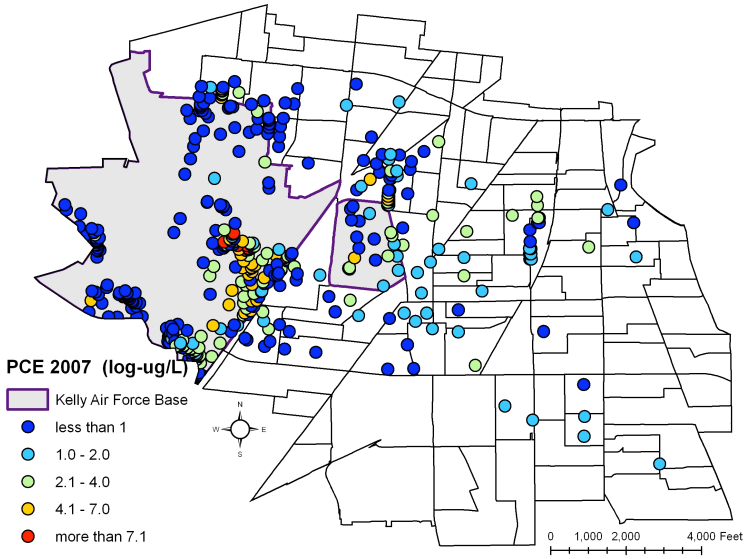

Figure A- 4: Spatial distribution of PCE well measurements in 2007.

2. Mean Trend Analysis: From the site-specific data, BMEGUI estimates the mean trend representing the trend of the log-transformed PCE distribution over space and time. The mean trend uses a smoothing range to attain temporal and spatially average data.

(a) Temporal Mean Trend: The overall trend of the data across the 10 year period is a decrease in PCE concentrations until 2002 when the level begin to rise. The solid line is the smoothed temporal trend, calculated from the raw temporal trend denoted by the dashed line.

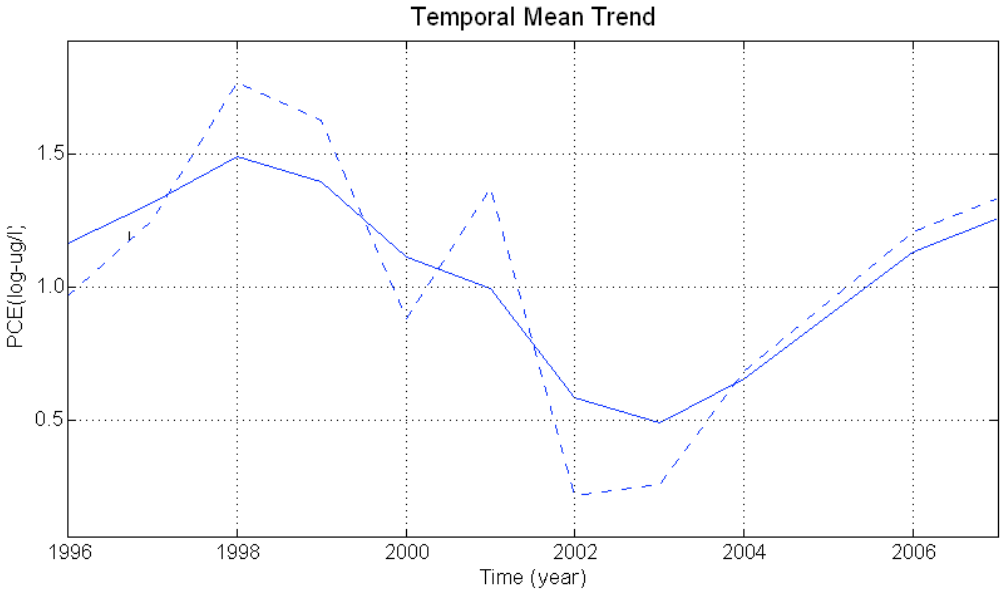

Figure A- 5: Smoothed temporal mean trend for PCE from 1997-2007.

(b) Spatial Mean Trend: In general, the highest concentrations are measured in the southeast section of the base and decrease north and east. This is a known source area for PCE contamination. The groundwater dominant pathway is from the northwest to the southeast.

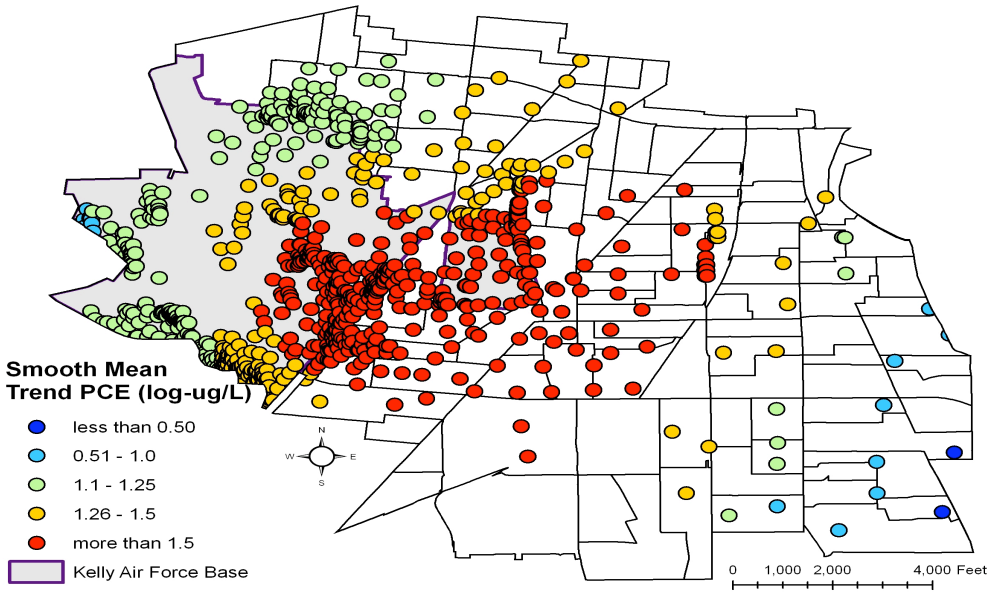

Figure A- 6: Smoothed spatial mean trend (log-ug/L)

3. Space-Time Covariance: The mean trend is removed from the log-transformed data resulting in a space-time random field of log-transformed mean-trend removed residential data. The resulting field is homogenous/stationary.

(a) Temporal Covariance: The temporal covariance indicates a strong relationship between two point across time. Chemical concentrations show

correlation even after 8 years. This points to the chemical properties of PCE, which does not readily degrade in groundwater. This may also suggest a continuous supply of PCE into the aquifer.

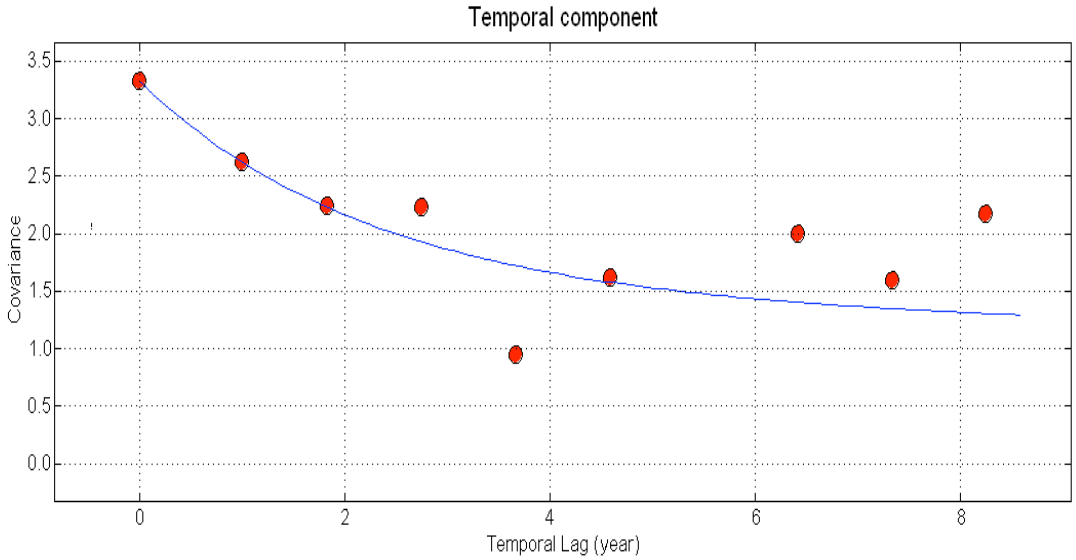

Figure A- 7: Temporal covariance of mean trend removed log-transformed PCE data.

(b) Spatial Covariance: The covariance is characterized by an exponential function showing a steep decline in correlation between monitoring well after 2500 feet. For monitoring wells farther than this distance, the PCE concentration shows no correlation.

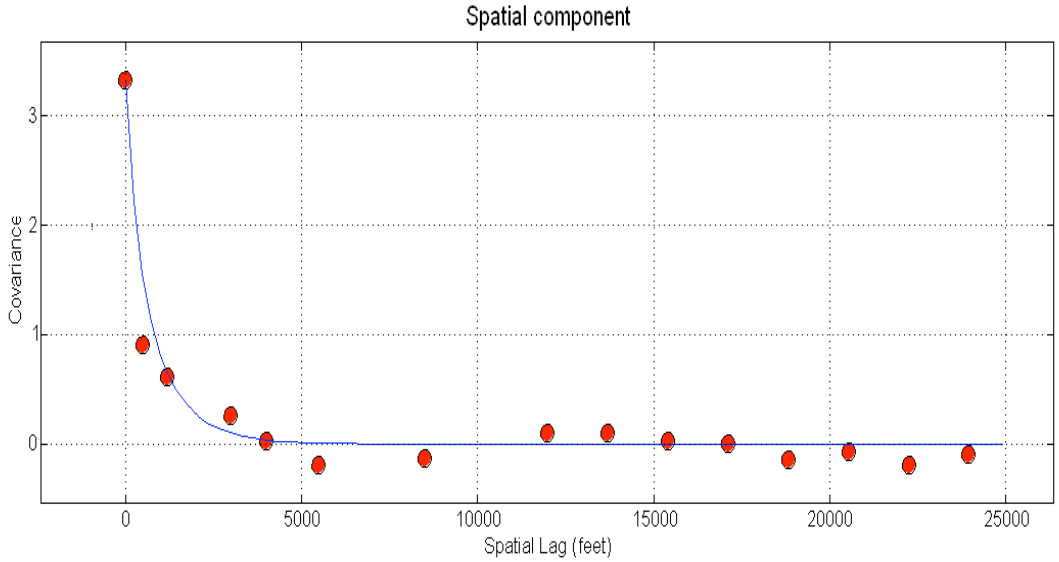

Figure A- 8: Spatial covariance of mean trend removed log-transformed PCE data.

4. Error Variance: In the error map, the blue sections are sites where there are measured data, and the error increases as a location becomes farther from a monitoring site. It is notable that the locations with the highest PCE concentrations have low associated error, attributing more confidence to the displayed values. Reference concentration maps are in Figure 8.

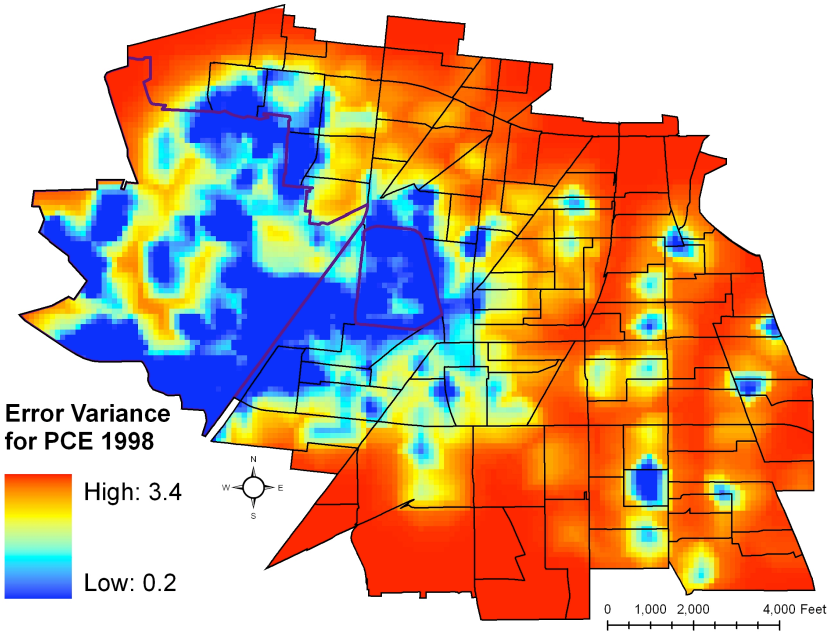

Figure A- 9: Error associated with 1998 PCE estimation map (log-ug/L squared).

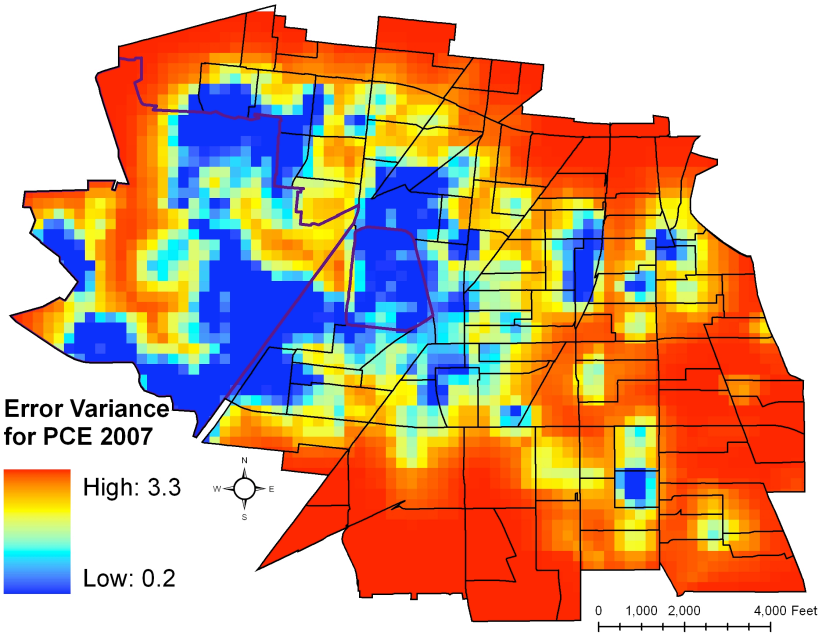

Figure A- 10: Error associated with 2007 PCE estimation map (log-ug/L squared).

REFERENCES

Abreu, L. D. V., & Johnson, P. C. (2005). Effect of vapor source− building separation and building construction on soil vapor intrusion as studied with a three-dimensional numerical model. *Environ.Sci.Technol, 39*(12), 4550-4561.

Agency for Toxic Substances and Disease Registry. (2006). *Health consultation: Endicott area investigation health statistics review, Endicott, Broome county, New York*. Atlanta, Georgia: U.S. Public Health Service.

Bozkurt, O., Pennell, K. G., & Suuberg, E. M. (2009). Simulation of the vapor intrusion process for nonhomogeneous soils using a three-dimensional numerical model. *Ground Water Monitoring and Remediation, 29*(1), 92-104.

Bureau of Economic Geology. (1983). *Geologic atlas of Texas, San Antonio sheet, scale 1:250,000.*

Carsel, R. F., & Parrish, R. S. (1988). Developing joint probability distributions of soil water retention characteristics. *Water Resources Research, 24*(5).

CDPHE. (2002). *Analysis of diagnosed vs. expected cancer cases in the vicinity of the Redfield plume area in southeast Denver county, 1979-1999.* Colorado Dept of Public Health and Environment.

Chan, W. R., Nazaroff, W. W., Price, P. N., Sohn, M. D., & Gadgil, A. J. (2005). Analyzing a database of residential air leakage in the United States. *Atmospheric Environment, 39*(19), 3445-3455.

Charbotel, B., Fevotte, J., Hours, M., Martin, J. L., & Bergeret, A. (2006). Case-control study on renal cell cancer and occupational exposure to trichloroethylene. part II: Epidemiological aspects. *Annals of Occupational Hygiene, 50*(8), 777.

Christakos, G., Bogaert, P., & Serre, M. L. (2001). *Temporal GIS: Advanced functions for field-based applications*. Berlin; New York: Springer pp. 217.

DiGiulio, D., Paul, C., Cody, R., Willey, R., Clifford, S., Kahn, P., et al. (2006). *Assessment of Vapor Intrusion in Homes Near the Raymark Superfund Site using Basement and Sub-Slab Air Samples.* Cincinnati, OH: U.S. Environmental Protection Agency.

Eaton, R., & Scott, A. (1984). Understanding radon transport into houses. *Radiat.Prot.Dosim, 7*(1-4), 251-253.

EerNisse, P. A., Steinmacher, S. J., Mehraban, T., Case, J. D., & Hanover, R. (2009). *Vapor intrusion mitigation system efficacy in residential communities surrounding hill air force base, Utah.* Air & Waste Management Association.

Eklund, B. M., & Simon, M. A. (2007). Concentration of tetrachloroethylene in indoor air at a former dry cleaner facility as a function of subsurface contamination: A case study. *Journal of the Air & Waste Management Association (1995), 57*(6), 753-760.

Environmental Quality Management, Inc. (2004). *User's guide for evaluating subsurface vapor intrusion into buildings*. Durham, NC: US Environmental Protection Agency—Office of Emergency and Remedial Response.

Ferguson, C., Krylov, V., & McGrath, P. (1995). Contamination of indoor air by toxic soil vapours: A screening risk assessment model. *Building and Environment, 30*(3), 375-383.

Fischer, D., & Uchrin, C. G. (1996). Laboratory simulation of VOC entry into residence basements from soil gas. *Environ.Sci.Technol, 30*(8), 2598-2603.

Fischer, M. L., Bentley, A. J., Dunkin, K. A., Hodgson, A. T., Nazaroff, W. W., Sextro, R. G., et al. (1996). Factors affecting indoor air concentrations of volatile organic compounds at a site of subsurface gasoline contamination. *Environ.Sci.Technol, 30*(10), 2948-2957.

Fitzpatrick, N. A., & Fitzgerald, J. J. (2002). An evaluation of vapor intrusion into buildings through a study of field data. *Soil and Sediment Contamination, 11*(4), 603-623.

Folkes, D., Wertz, W., Kurtz, J., & Kuehster, T. (2009). Observed spatial and temporal distributions of CVOCs at Colorado and New York vapor intrusion sites. *Ground Water Monitoring & Remediation, 29*(1), 70-80.

Garbesi, K., & Sextro, R. G. (1989). Modeling and field evidence of pressure-driven entry of soil gas into a house through permeable below-grade walls. *Environmental Science & Technology, 23*(12), 1481-1487.

Hers, I., & Zapf-Gilje, R. (2003). Evaluation of the johnson and ettinger model for prediction of indoor air quality. *Ground Water Monitoring and Remediation, 23*(2), 119-133.

Hers, I., Zapf-Gilje, R., Evans, D., & Li, L. (2002). Comparison, validation, and use of models for predicting indoor air quality from soil and groundwater contamination. *Soil and Sediment Contamination, 11*(4), 491-527.

Hodgson, A. T., Garbesi, K., Sextro, R. G., & Daisey, J. M. (1992). Soil-gas contamination and entry of volatile organic compounds into a house near a landfill. *Journal of the Air & Waste Management Association, 42*(3), 277-283.

Hun, D. E., Morandi, M. T., Corsi, R. L., Siegel, J. A., & Stock, T. H. (2008). Exposure and risk disparities between Mexican-American and non-Hispanic white populations in Houston. Paper presented at the *Proceedings from the 11 The International Conference on Indoor Air Quality and Climate Indoor Air 2008,* 1-8.

HydroGeoLogic, I. (2007). *Final semiannual compliance plan report: January through june 2007, former Kelly AFB, San Antonio, TX* No. F41624-03-D-8602-0065. San Antonio, TX: Air Force Real Property Agency.

Johnson, P. C. (2002). Identification of critical parameters for the Johnson and Ettinger (1991) vapor intrusion model. *American Petroleum Institute Technical Bulletin,*17-38.

Johnson, P. C. (2005). Identification of application-specific critical inputs for the 1991 Johnson and Ettinger vapor intrusion algorithm. *Ground Water Monitoring and Remediation, 25*(1), 63-78.

Johnson, P. C., & Ettinger, R. A. (1991). Heuristic model for predicting the intrusion rate of contaminant vapors into buildings. *Environmental Science & Technology, 25*(8), 1445-1452.

Johnson, P.C., Ettinger, R., Kurtz, J., Bryan, R., & Kester, J. (2009). Empirical assessment of ground water-to-indoor air attenuation factors for the CDOT-MTL denver site. *Ground Water Monitoring and Remediation, 29*(1), 153-159.

Klepeis, N. E., Nelson, W. C., Ott, W. R., Robinson, J. P., Tsang, A. M., Switzer, P., et al. (2001). The national human activity pattern survey (NHAPS): A resource for assessing exposure to environmental pollutants. *Journal of Exposure Analysis and Environmental Epidemiology, 11*(3), 231-252.

Kliest, J. (1989). Relationship between soil contaminated with volatile organic compounds and indoor air pollution. *Environment International, 15*(1), 419.

Little, J. C., Daisey, J. M., & Nazaroff, W. W. (1992). Transport of subsurface contaminants into buildings. *Environmental Science & Technology, 26*(11), 2058-2066.

McDonald, G. J., & Wertz, W. E. (2007). PCE, TCE, and TCA vapors in subslab soil gas and indoor air: A case study in upstate New York. *Ground Water Monitoring & Remediation, 27*(4), 86-92.

Meng, Q. Y., Turpin, B. J., Korn, L., Weisel, C. P., Morandi, M., Colome, S., et al. (2004). Influence of ambient (outdoor) sources on residential indoor and personal PM2.5 concentrations: Analyses of RIOPA data. *Journal of Exposure Science and Environmental Epidemiology, 15*(1), 17-28.

Millington, R., & Quirk, J. (1961). Permeability of porous solids. *Transactions of the Faraday Society, 57*, 1200-1207.

Mills, W. B., Liu, S., Rigby, M. C., & Brenners, D. (2007). Time-variable simulation of soil vapor intrusion into a building with a combined crawl space and basement. *Environ.Sci.Technol, 41*(14), 4993-5001.

Mittal, A. K. (2005). *Groundwater contamination: DOD uses and develops a range of remediation technologies to cleanup military sites*. Washington, DC: US General Office of Accountability.

Nazaroff, W. W. (1992). Radon transport from soil to air. *Reviews of Geophysics, 30*(2).

Nazaroff, W. W., Lewis, S. R., Doyle, S. M., Moed, B. A., & Nero, A. V. (1987). Experiments on pollutant transport from soil into residential basements by pressure-driven airflow. *Environmental Science & Technology, 21*(5), 459-466.

Olson, D. A., & Corsi, R. L. (2001). Characterizing exposure to chemicals from soil vapor intrusion using a two-compartment model. *Atmospheric Environment, 35*(24), 4201-4209.

Pennell, K. G., Bozkurt, O., & Suuberg, E. M. (2009). Development and application of a three-dimensional finite element vapor intrusion model. *Journal of the Air & Waste Management Association, 59*(4), 447-460.

Pepelko, W. E., & Withey, J. R. (1985). Methods for route-to-route extrapolation of dose. *Toxicol.Ind.Health, 1*(4), 153-175.

Provoost, J., Reijnders, L., Swartjes, F., Bronders, J., Seuntjens, P., & Lijzen, J. (2009). Accuracy of seven vapour intrusion algorithms for VOC in groundwater. *Journal of Soils and Sediments, 9*(1), 62-73.

Radian Corporation. (1984). *Installation restoration program: Phase II stage 1 field evaluation, Kelly AFB, Texas* No. 84—212—027—03—04). Brooks AFB, Texas: US Air Force Occupational and Environmental Health Laboratory.

Renner, R. (2002). A case of the vapors. *Scientific American, 287*(1), 27.

Robinson, A. L., Sextro, R. G., & Riley, W. J. (1997). Soil-gas entry into houses driven by atmospheric pressure fluctuations—the influence of soil properties. *Atmospheric Environment, 31*(10), 1487-1495.

Sanders, P. F., & Hers, I. (2006). Vapor intrusion in homes over gasoline-contaminated ground water in Stafford, New Jersey. *Ground Water Monitoring and Remediation, 26*(1), 63-72.

Schaap, M. G. (1998). Neural network analysis for hierarchical prediction of soil hydraulic properties. *Soil Science Society of America Journal, 62*(4), 847.

Schreuder, W. A. (2006). *Uncertainty approach to the Johnson and Ettinger vapor intrusion model* No. 072681998). Chicago, Il: NATIONAL GROUND WATER ASSOCIATION.

Schuver, H. (2007). Intrusion: Risks and challenges. *Air & Waste Management Association,*6-9.

Serre, M. L., Carter, G., & Money, E. (2004). Geostatistical space/time estimation of water quality along the Raritan river basin in New Jersey. *Computational Methods in Water Resources, Part 2*, 13–17.

Soil Survey Staff, Natural Resources Conservation Service, United States Department of Agriculture (2009). Soil Survey Geographic (SSURGO) Database for Bexar County, Texas. Available online at http://soildatamart.nrcs.usda.gov accessed 10/24/2009.

Spengler, J., & Sexton, K. (1983). Indoor air pollution: A public health perspective. *Science, 221*(4605), 9-17.

Tillman, F. D., & Weaver, J. W. (2006). Uncertainty from synergistic effects of multiple parameters in the Johnson and Ettinger (1991) vapor intrusion model. *Atmospheric Environment, 40*(22), 4098-4112.

U.S. EPA. (1992). *Air/Superfund national technical guidance series: Assessing potential indoor air impacts for superfund sites* No. EPA-451/R-92-002). Research Triangle Park, NC: U.S. EPA.

US EPA. (2008). *U.S. EPA's vapor intrusion database: Preliminary evaluation of attenuation factors, draft*. Washington, DC: U.S. Environmental Protection Agency.

van Genuchten, M. T. (1980). A closed-form equation for predicting the hydraulic conductivity of unsaturated soils. *Soil Sci.Soc.Am.J, 44*(5), 892-898.

Yamamoto, N., Shendell, D. G., Winer, A. M., & Zhang, J. J. (2009). Residential air exchange rates in three major US metropolitan areas: Results from the RIOPA study 1999-2001. *Indoor Air, 9999*(999A).